Layered titanate nanostructures: perspectives for industrial exploitation

2015 Transl. Mater. Res. 2 015003

(http://iopscience.iop.org/2053-1613/2/1/015003)

IOP Publishing Transl. Mater. Res. 2 (2015) 015003 doi:10.1088/2053-1613/2/1/015003

Translational Materials Research

PAPER

Layered titanate nanostructures: perspectives for industrial exploitation

RECEIVED
29 January 2015

REVISED
30 March 2015

ACCEPTED FOR PUBLICATION
31 March 2015

PUBLISHED
27 April 2015

Krisztián Kordás[1], Melinda Mohl[1], Zoltán Kónya[2,3], Ákos Kukovecz[2,4]

[1] Department of Electrical Engineering, Microelectronics and Materials Physics Laboratories, University of Oulu, Oulu FIN-90014, Finland
[2] Department of Applied and Environmental Chemistry, University of Szeged, Faculty of Science and Informatics, Rerrich Béla tér 1., H-6720 Szeged, Hungary
[3] MTA-SZTE Reaction Kinetics and Surface Chemistry Research Group, Rerrich Béla tér 1., H-6720 Szeged, Hungary
[4] MTA-SZTE 'Lendület' Porous Nanocomposites Research Group, Rerrich Béla tér 1., H-6720 Szeged, Hungary

E-mail: kakos@chem.u-szeged.hu

Keywords: titanate, scale-up, nanotube, layered materials

Abstract

Anisotropic titanate nanostructures can be synthesized by an environmentally benign, cost efficient and scalable process, the alkaline hydrothermal recrystallization of TiO_2 with yields approaching 100%. Their chemistry offers more variety than that of TiO_2 nanoparticles and promising preliminary results were already achieved on them in the fields of adsorption, catalysis and energy storage. In this review we first discuss the structure, synthesis and functionalization options of titanate nanotubes and nanowires, then the issues related to their industrial scale production, and finally present selected examples of their currently available applications.

1. Introduction

Nanostructures of layered titanates have evolved from a laboratory curiosity into a standalone subfield of nanotechnology in the past 15 years. Their simple and readily scalable synthesis and favorable application potential render them good choices for several industrial applications. Relevant industrial sectors are (i) paints and coatings, (ii) pharmaceutics, (iii) electronics, (iv) energy storage and (v) photocatalysis.

TiO_2 nanoparticles were among the first materials synthesized <100 nm in diameter with monodisperse size distribution [1]. In 1998 Kasuga *et al* converted TiO_2 into a layered multiwall nanotube by hydrothermal treatment, thus opening a new field of research that has been evolving rapidly since then [2, 3]. An ISI Web of Science topic search for 1D titanate nanomaterials finds over 10 000 related publications and reveals an increasing recent scientific interest: a new paper is published almost daily in this field now. In-depth reviews on their general aspects [4] as well as their synthesis [5], growth mechanism [6] and photocatalytic applicability [7] are available. 2D TiO_2 nanosheets are also extensively studied since the onset of the graphene revolution. A recent review on this subject was published by Wang and Sasaki [8].

In this review we will first define our topic by showing the landscape of the presently available nanostructures containing titanium and oxygen. Then we introduce the properties and synthesis methods of layered titanates following the work of Bavykin and Walsh [9]. This will be followed by the discussion of the issues related to the industrial scale production of 1D trititanate nanomaterials. The second part of the paper will give an overview of their potential applications and provide examples of commercial trititanate nanoproducts.

2. Fundamental properties

This section will introduce layered titanate nanomaterials by discussing their structure and basic properties.

2.1. Titania phases

The three stable allotropes of TiO_2 at ambient conditions are anatase (tetragonal), rutile (tetragonal) and brookite (orthorhombic). In addition, TiO_2 exists in three more metastable forms TiO_2 (B), TiO_2 (H), TiO_2 (R) and five

phases formed at high pressure only [10]. TiO_2 is among the most common nanomaterials today. It is typically produced in the form of isotropic nanoparticles and used for photocatalysis, photovoltaics, coatings and sensors.

Regardless of the exact crystal structure, it is important to make a clear distinction between TiO_2 and titanate phases. The former are mixed ionic (70%)—covalent (30%) wide bandgap indirect semiconductors [11] with little structural flexibility and a composition of Ti:O = 1:2 (although oxygen deficient structures can easily be obtained), whereas titanates are the salts of polytitanic acids. Titanates feature a negatively charged framework consisting of TiO_6 octahedra sharing vertexes, edges or faces. Their band gap is wider, their framework charge is compensated by cations that can be exchanged by conventional ion exchange processes, and their Ti:O ratio can vary considerably depending on the exact formation conditions.

The most important titanates are perovskites and layered titanate materials. Perovskites are crystals with a structure analogous to the mineral $CaTiO_3$ (ABX_3 structure, where A and B are cations, A ions are much larger than B ions and X is a common anion). $BaTiO_3$ and PZT ($Pb[Zr_xTi_{1-x}]O_3$) are two common, industrially important perovskites used extensively because of their ferroelectric properties [12–14]. One the other hand, layered titanates are the materials that readily yield highly anisotropic lamellar nanostructures, therefore, we will focus on them from now on and refer to some excellent reviews for more information on TiO_2 [15–18] and perovskite nanostructures [19–21].

The typical chemical formula of layered titanates is $M_{2n}Ti_mO_{2m+n} \bullet H_2O$ where M is a positively charged species: an alkali ion (Na^+ or K^+) directly after the hydrothermal synthesis, H^+ after washing and practically any cation after appropriate ion exchange. Therefore, layered titanate nanostructures are best considered to be salts of polytitanic acids, for example $Na_2Ti_3O_7$ as sodium trititanate, $H_2Ti_4O_9$ as tetratitanic acid, $K_2Ti_5O_{11}$ as potassium pentatitanate etc. These structures are all monoclinic, feature three steps of corrugated edge-sharing TiO_6 octahedral layers and are very similar to each other, making unambiguous XRD phase identification rather challenging. The other structural possibility is that of dititanic acid $H_2Ti_2O_4(OH)_2$ and the closely related lepidocrocite $H_xTi_{2-x/4}[]_{x/4}O_4(OH)_2$ where [] denotes a vacancy [22]. Both of these are orthorhombic structures where layers are made up of continuous planar arrays of edge-sharing TiO_6 octahedra.

2.2. Layered titanate structure and morphology

Considerable controversy can be observed in the literature concerning the exact crystalline structure of titanate nanoobjects [22–30]. The XRD profiles of such small particles experience line broadening, and when this effect is combined with the intrinsic similarity of the diffractograms of various titanates (e.g. trititanate, pentatitanate, nonatitanate, lepidocrocite etc.) it makes accurate Miller indexing and crystalline phase identification difficult. Moreover, layered titanates readily transform into each other, and the same starting material can yield multiple metastable end products upon thermal annealing depending on the cations of the starting material, the heating rate and the annealing time and temperature.

In spite of these ambiguities it is safe to say that the first product of the alkaline hydrothermal synthesis reaction is a layered nanostructured titanate material that is well approximated as sodium trititanate ($Na_2Ti_3O_7$). This structure is largely preserved during washing to neutral pH. Subsequent chemical treatment or prolonged storage yields a mixture of titanate phases.

The layered structure of metatitanic acid offers zero, one and two dimensional possible nanoparticle morphologies as summarized in figure 1. The two most important ones are 1D titanate nanotubes and nanowires. Nanotubes resemble a rolled-up carpet measuring 50–200 nm in length, 4–8 nm inner and 8–15 nm outer diameter and consist of multiple (4–7) walls separated by approximately 1 nm, which corresponds to the 0.96 nm (1 0 0) interplanar distance of $Na_2Ti_3O_7$. The two characteristic morphological differences between titanate nanotubes and the more well-known multiwall carbon nanotubes are that (i) the cross section of the former is a spiral instead of a Russian doll array, and (ii) the inner channel of titanate nanotubes is readily accessible, whereas that of the carbon nanotubes is closed by half-fullerene domes. Titanate nanowires are formed of $Na_2Ti_3O_7$ sheets arranged into 300–1500 nm long and 30–60 nm thick structures with a roughly rectangular cross section and no hollow inner channel.

In addition to these dominant morphologies, many other titanate nanostructures were also observed. These are mostly either nanosheet based structures like flowers [31] or very thin sheets [32], or quasi-isomorphic particles measuring 10–30 nm in diameter and exhibiting a cuboid or spiral structure [33].

2.3. Interconversions of nanostructured titanates

Spontaneous phase transformations can occur even when stored in ambient conditions. They can be accelerated by the humidity of the storage atmosphere and, in particular, by the pH of the storage media, since layered titanates do not tolerate mineral acids well. Sui *et al* have recently demonstrated that the pH-decrease induced gradual transformation of the $H_2Ti_2O_5$ phase in hydrogenotitanate/titania composite nanotubes affects the distribution and electrocatalytic properties of Pt nanoparticles supported on the titanate nanostructure [34]. Acid resistance can be improved by iron ion exchange according to Marinkovic *et al* [35]. Hydrothermally synthesized titanate

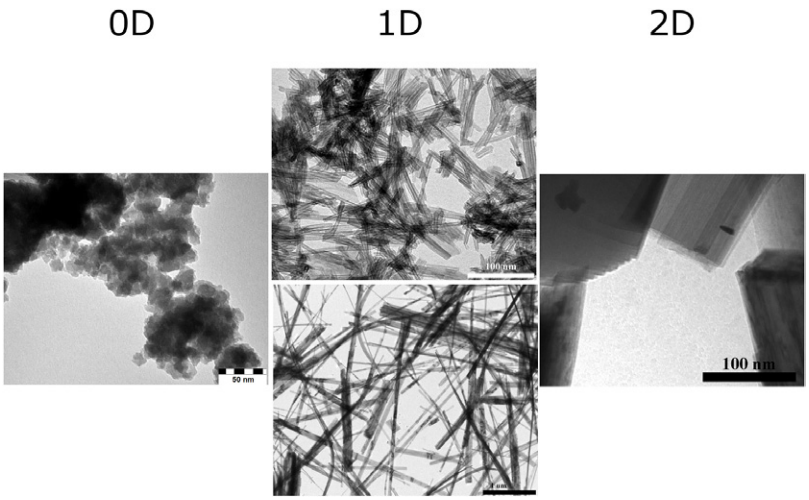

Figure 1. Characteristic TEM images of layered titanate morphologies. 0D quasi-isomorphic particles (0D), 0D nanotubes (1D, top) and nanowires (1D, bottom) and 2D stacked nanosheets (2D).

nanotubes spontaneously convert into rhombic and spindle-shape anatase nanoparticles in 10 min in supercritical water [36]. Mao and Wong demonstrated that lepidocrocite titanate nanotubes and nanowires transform into anatase nanoparticles and nanowires, respectively, in neutral solution [37].

Titania nanostructures can also be converted into each other deliberately by multiple processes [38]. The simplest of all is the thermal treatment that induces the transformation to TiO_2(B) (400 °C), anatase (700 °C) and then rutile (1000 °C). Kuo *et al* even reported on a trititanate to TiO_2(B) transformation at 300 °C [39]. The details of this transformation were investigated by Morgado *et al* [40]. The open inner channel of nanotubes is preserved up to 400 °C, then the structure gradually collapses into shorter nanorods [41–44]. Nanowires can withstand temperatures up to 1000 °C without the loss of their fibrous morphology, and then they convert into more isotropic fragments [45]. It is interesting to note that the phase transformation temperature is heavily influenced by the ion exchange, doping level and eventual nanoparticle decoration of the layered titanate starting material [46]. Beuvier *et al* established a ternary morphological diagram that summarizes the relative proportion of nanotubes, nanospheres and nanoribbons in heat treated H-form trititanates [47].

Fine tuning the temperature and duration of the alkaline hydrothermal synthesis can be used to either stop the process when titanate nanotube concentration is at a maximum, or let it run further and allow nanotubes to spontaneously merge into titanate nanowires [48]. Bavykin *et al* have shown nanowires to be the most stable morphology under these experimental conditions: the system gains approximately 20 kJ · mol^{-1} by the nanowire formation [49]. Nanotubes can also be converted directly into anatase and/or rutile nanoparticles by long (several months) exposure to mineral acids below 100 °C. Ultrasonic or mechanochemical energy transfer to titanate nanotubes first breaks them into shorter fragments, then these are morphed into titanate nanosheets. Further energy input yields quasi-isotropic anatase and finally, rutile nanoparticles.

Even though titanate nanowires are thermodynamically favored over nanotubes, it is also possible to transform nanowires into nanotubes by a non-equilibrium process. Kozma *et al* have demonstrated that the careful engineering of mechanochemical process parameters (11 mJ · hit^{-1}, 892 J · g^{-1} cumulative energy) in a high energy planetary ball causes titanate nanosheets to delaminate from nanowires upon ball impact, but prevents their phase transformation into anatase or rutile [50]. The system is thus quenched in a high-energy metastable state that can stabilize into a local energy minimum if the nanosheets roll up into nanotubes.

Nanotube delamination into nanosheets [51] can also be achieved by ultrasonication [52] or acid treatment [53]. Titania nanosheets can then be converted into TiO_2 thin film hydrothermally [54].

Titanates can be converted into perovskites that inherit the 1D morphology of the parent sacrificial template. Ca-, Sr- and Ba- titanate microstructures were created this way by Li *et al* [55] from sodium trititanate nanofibers and by Cao *et al* from potassium tetratitanate nanowhiskers [56].

2.4. Titanate nanomaterial properties

Layered titanate nanomaterials are white powders when synthesized correctly. Discolorations can be caused either by metallic impurities (e.g. iron ions from the steel walls of the synthesis vessel or piping) or oxygen deficiency. The latter can occur spontaneously when heating the material in an inert or reducing atmosphere. The density of titanate nanotubes as measured by He pycnometry is 3.12 g · cm^{-3} [57]. The main difference between bulk and nanostructured titanates is that the inner layers are not accessible in bulk; therefore, delamination and layer

Table 1. An overview of titanate nanomaterial properties.

	Nanotube	Nanowire	Nanosheet
Diameter or thickness	8–15 nm [2, 9, 64]	5–300 nm [65–67]	< 10 nm [9]
Length or lateral dimensions	Up to several micrometers [9]	Up to several micrometers [65, 66]	> 100 nm [9]
Band gap	3.3–3.9 eV [52, 61, 68, 69]	3.4–3.6 eV [68, 70]	3.8 eV [8, 52]
Specific surface area	50–400 $m^2 \cdot g^{-1}$ [2, 58, 59, 64, 71]	18–130 $m^2 \cdot g^{-1}$ [72–74]	240–380 $m^2 \cdot g^{-1}$ [75, 76]
Young's modulus	n.a.	14–46 GPa [77, 78]	n.a.
Electrical conductivity	$1.5 \cdot 10^{-6}$–$7.9 \cdot 10^{-7}$ $S \cdot cm^{-1}$ [62, 63]	~10^{-7} $S \cdot cm^{-1}$ for porous films of NWs and ~10^{-1} $S \cdot cm^{-1}$ for individual belts [79, 80]	10^{-10} $S \cdot cm^{-1}$ for films of nanosheets [81]

scrolling do not occur. The other notable differences are decreased band gap energy, increased specific surface area and lower melting point in nanomaterials (table 1). The difference between monoclinic and orthorhombic nanoscale titanates is in the arrangement of the edge-sharing TiO_6 octahedra along the *c*-axis (i.e. around the nanotube perimeter). In monoclinic structures, there are three or four repeating octahedral units that are connected in their corners with the adjacent repeating units. In the case of the orthorhombic layered titanate nanotubes, the edge-sharing octahedra are continuing in a linear fashion. Accordingly, the surface of the monoclinic nanotubes is corrugated around the perimeter, while smooth for the orthorhombic ones. Note that the surface is corrugated along the tube axes for both kinds of crystal structure [9].

The BET specific surface area of titanate nanotubes is between 200–300 $m^2 \cdot g^{-1}$ when calculated from the most common nitrogen adsorption isotherm. It is also possible to estimate the surface area from water adsorption isotherms evaluated by the Guggenheim–Anderson–de Boer (GAB) equation [58], but this method tends to overestimate the surface (approximately 350 $m^2 \cdot g^{-1}$) because water adsorption is significantly more complex on the hydrophilic titanate surface than nitrogen sorption [59]. Surface area values calculated from geometrical models are closer to the BET than to the GAB values. The specific surface area of titanate nanowires is below 50 $m^2 \cdot g^{-1}$, the exact value depends on the aspect ratio of the nanowires.

The exfoliation of layered protonic titanates yields 2D lepidocrocite TiO_2 nanosheets [8] with a band gap (3.84 eV) blue shifted compared to anatase TiO_2 (3.2 eV). Rolling these sheets up into nanotubes results in additional changes in the electronic structure [60]. An experimental study on the UV-Vis absorption properties of titanate nanotube suspensions revealed a band gap of 3.87 eV [61]. The band gap energy was found to be independent of the internal diameter of the nanotubes.

The electrical conductivity of titanate nanotubes is generally higher than that of TiO_2 nanoparticles (approx. 10^{-9} $S \cdot cm^{-1}$) because conduction in nanotubes is largely governed by proton mobility [62]. Consequently, their conductivity is sensitive to humidity and temperature. A base conductivity of $5.5 \cdot 10^{-6}$ $S \cdot cm^{-1}$ at 30 °C was found to increase to $1.5 \cdot 10^{-5}$ $S \cdot cm^{-1}$ upon heating to 130 °C and then drop to $7.9 \cdot 10^{-7}$ $S \cdot cm^{-1}$ at 225 °C [62] because of the loss of water from the nanotube pores [63]. This latter value corresponds to the electron conductivity of titanate nanotubes.

Layered titanate nanostructures are hydrophilic materials. They can be filtered into self-supporting membranes similar to carbon nanotube buckypaper by dead-end filtration [66, 82–84]. Miyauchi and Tokudome have succeeded in creating transparent super-hydrophilic films featuring a water contact angle of 0 degrees under UV illumination [85]. Water sorption on titanate nanowires was extensively studied by Haspel *et al* using broadband dielectric spectroscopy [86]. Three relaxation processes plus ionic conduction were found in the 10 mHz–10 MHz frequency window. The conductivity variation originates from the increasing charge carrier concentration, middle frequency relaxations have a common interfacial origin and the high frequency loss process is due to the orientation relaxation of a dipolar moiety.

Bo *et al* have recently measured the mechanical properties of sodium trititanate nanowires [78]. The effective Young's modulus of $Na_2Ti_3O_7$ nanowires was found to be independent of the wire length and ranged from 21.4 GPa to 45.5 GPa, with an average value of 33 $\pm$ 7 GPa. The yield strength of the $Na_2Ti_3O_7$ was 2.7 $\pm$ 0.7 GPa. This result agrees qualitatively with the earlier work of Chang *et al* who found Young's moduli in the 14–17 GPa range for titanate nanowires [77].

H-form titanate nanotubes are solid acids possessing both Bronsted and Lewis acid sites [87–89]. Kitano *et al* have shown that the Bronsted acid strength of titanate nanotubes is higher than that of the corresponding nanosheets and attributed the difference to the lattice distortion due to the scrolling of the lamellar titanate sheet [90]. There is a lack of standardized pKa data on titanate nanostructures in the literature. Available works typically use titration [89], thermogravimetry or adsorption (methylene blue [91], pyridine [87], CO_2 [92]) measurements to make smaller/larger type comparisons between the acidities of samples included in a particular study.

3. Chemistry of titanate nanostructures

This section introduces the chemistry of titanate nanostructures.

3.1. Synthesis

The alkaline hydrothermal synthesis discovered in 1998 by Kasuga *et al* has rapidly become the dominant non-templated method for producing layered titanate nanomaterials. Its main advantages are the use of cheap raw materials (TiO_2, NaOH, water), the good nanomaterial yield and the possibility to control the product morphology by tuning the composition of the reaction mixture.

In a typical titanate nanotube synthesis 2 g of anatase TiO_2 is mixed into 140 ml 10 M NaOH aqueous solution until a white suspension is obtained, then the suspension is aged in a closed, Teflon-lined autoclave at 130 °C for 72 h without shaking or stirring. The product is then washed with deionized water to reach pH 8 at which point the slurry is filtered and the titanate nanotubes are dried in air.

The recipe for titanate nanowires is very similar, since titanate nanotubes are actually intermediates in the TiO_2 to titanate nanowire recrystallization process. Therefore, the same experimental setup and reaction mixture should be used, but the process must be intensified. This can be achieved by increasing the reaction temperature to approximately 180 °C, increasing the reaction time to approximately 1 week or agitating the system by e.g. rotating the whole autoclave around its short axis.

The alkaline hydrothermal synthesis is very robust: layered anisotropic titanate nanostructures can be prepared by using a broad range of TiO_2 sources [93–95] and compositions, different bases [69, 96, 97], reaction times, temperatures and post-synthetic treatments. However, changing the recipe will affect the properties of the product mixture (e.g. nanotube:nanowire ratio, diameter and length distribution) [46, 98–104]. Moreover, Dawson *et al* argued that trititanate nanotubes are formed exclusively from the anatase fraction of the starting material, whereas the rutile component produces trititanate sheets and plates [105]. However, this hypothesis is yet to be confirmed since there are reports on the successful synthesis of trititanate nanotubes from e.g. P25 [106] and tetraisopropyl orthotitanate as well [107].

The main drawback of the process is the need to use pressurized equipment. Bavykin *et al* were able to overcome this issue by refluxing TiO_2 in an aqueous mixture of NaOH and KOH for 48 h at 100 °C. Similar to the hydrothermal process, the product distribution could be tuned by the reaction conditions [108].

3.2. Modification

Layered titanate nanomaterials have a rich chemistry and offer some modification possibilities not available on TiO_2.

Both titanate nanotubes and nanowires have exchangeable cations occupying positions on their surface as well as between the titanate layers. Indeed, ion exchange is an integral part of the synthesis process itself, since the majority of Na^+ ions from the crystallized nanostructure are replaced by protons during washing. Monovalent cations are exchanged readily and almost quantitatively (that is, in the formula $Me_xH_{2-x}Ti_3O_7$, x can be close to 2), whereas cations with multiple positive charges are more difficult to exchange because they introduce extra stress into the lattice [109]. It has also been shown that the temperature-induced transformation of titanates into anatase can be hindered by the presence of metallic cations [99–101, 110]. Interestingly, the apparent rate of intercalation of alkaline metal cations is independent of the ion size, and the d_{200} interplanar distance of the resulting structures is also almost identical for all alkaline metals (0.88 nm for H-form, 1.18 nm for alkaline forms) [111].

It is possible to add extra functionality to layered titanate nanostructures by exploiting their ion exchange properties. Silver containing titanate nanotubes exhibit antimicrobial properties [112], Cd^{2+} and noble metal ions can be converted into CdS [113, 114] or metallic (e.g. Au, Rh) [115, 116] nanoparticles that decorate the nanotube surface and open up (photo)catalytic application possibilities, and cations can also serve as bridgeheads for further surface functionalization reactions, e.g. for tuning the hydrophilic/hydrophobic balance by anchoring fatty acid ions to surface cations. Hydrophobization is also possible by cationic surfactants like cetyl-trimethylammonium bromide [117] or poly(diallyldimethylammonium) chloride [118].

The modifiable structure of layered titanates combined with the possibility to transform them into anatase or rutile by thermal treatment renders them excellent precursors of doped TiO_2. An interesting recent application is the synthesis of Co doped single crystalline rutile from ion exchanged titanate nanotubes by Forró *et al* [119]. Their material showed metallic behavior below 50 K even though the Co^{2+} dopant concentration was only $5 \cdot 10^{19}$ cm^{-3}. It is likely that the same synthesis approach can be used for growing a large variety of doped TiO_2 single crystals. Co^{2+} doping was also found to introduce a room temperature hysteresis loop into the magnetic properties of the doped nanotubes [120].

Although ion exchange or nanoparticle deposition onto the surface are often referred to as ‘doping’ in the literature [121], actually, substitutional and interstitial doping of layered titanate nanomaterials correspond to replacing either the framework Ti sites by heteroatoms, or to inserting extra atoms into the titanate framework,

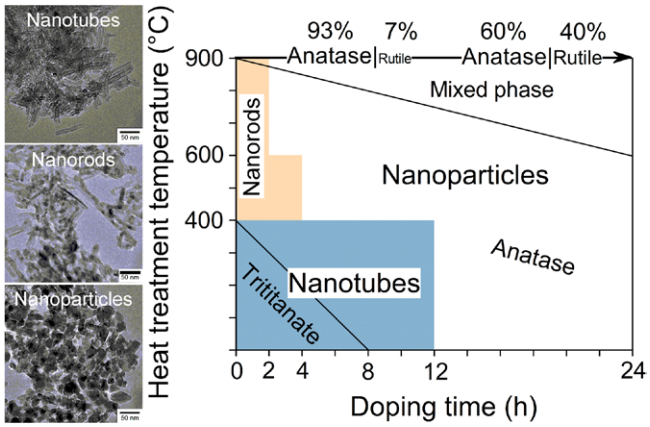

Figure 2. Variation of the morphology and crystalline phase of nitrogen-doped titanium-oxide nanostructures with nitrogen dotation (NH_3 exposure) duration and calcination temperature. Reproduced from [131] with permission of the Royal Society of Chemistry.

respectively. Unfortunately, experimentally confirmed information on the substitutional or interstitial nature of the doping is scarcely available in the literature. Hu *et al* reported XPS evidence for interstitial N-doping on the basis of observing both Ti–O–N and Ti–N–O linkages [122]. According to Wu *et al* both interstitial N positions and new Ti–N bonds can appear in the lattice of titanate nanofibers depending on the synthesis route [123]. Chang *et al* studied the details of N-doping in the thermal transformation of ammonium trititanate nanotubes and found evidence for the formation of interstitial NH_2 species after the dehydrogenation of NH_3 [124]. Diaz-Guerra *et al* have synthesized Cr^{3+} doped titanate nanotubes and nanoribbons and interpreted near infrared emission data as indication of interstitial chromium incorporation between the titanate layers [125]. Evidence for framework Ti substitution was provided by Song *et al* for Mn, Cr and Cu in trititanate nanotubes [126] and by He *et al* for Zr doped $Na_2Ti_4O_9$ nanobelts [127].

N-doped TiO_2 [128] can be synthesized by calcining NH_4^+ exchanged titanate nanostructures in inert gas [129] or H-form titanate nanowires in ammonia flow above 600 °C [130]. Pt and Pd nanoparticles were deposited on the doped product to yield a material with appreciable photocatalytic water splitting ability [123]. The record lowest temperature for N-doping was reported by Buchholcz *et al* to be 200 °C [131]. This latter example is particularly interesting because the titanate structure is preserved during doping, and the user can decide later if a phase change to doped anatase or rutile is desirable. Phase and morphology changes are summarized in the simplified phase map in figure 2. Other dopants reported in the literature are e.g. Fe [132], Zn [133], Mn [121, 134], La_2O_3 [135], Nb [136], Cu [137, 138], Ni [139] and Ho-Yb [140].

The presence of surface –OH groups on layered titanates makes it possible to functionalize them by covalent chemistry. The most feasible route is the controlled hydrolysis of trialkoxysilanes (e.g. $Si(EtO)_3R$) in the presence of titanates in anhydrous solvents [141]. This anchors the R chain onto the titanate by a strong Ti–O–Si–C bond. The primary use of this reaction is covalent hydrophobization, however, if the R group is reactive enough then it can also serve as a bridgehead for further organic functionalization steps and subsequent polymer grafting for nanocomposite applications [142–144]. The surface –OH groups can enter an esterification reaction with carboxylic acids in anhydrous alcohol [145].

Covalent functionalization is beneficial when anisotropic layered titanates are used as polymer fillers. Brnardic *et al* reported 7 °C higher glass transition temperature and 10.4% higher storage modulus in epoxy composites loaded with 3 wt% silanized titanate nanotubes [143].

4. Scaling issues

Let us now review the issues related to scaling layered titanate synthesis up to a commercial level.

The global production of metallic titanium sponge today is above 200 000 metric tons per year. Its main ores are anatase or rutile TiO_2 and ilmenite ($FeTiO_3$) which are mined in significantly larger quantities (combined world production over 7 million metric tons/year) because of the many uses of TiO_2 besides reduction to titanium metal. Layered titanates can be produced directly from TiO_2 cost-effectively (below 2 USD kg^{-1}), therefore, they rank among the potentially cheapest commercially available nanomaterials.

[5] None of the authors are officially affiliated with Auro-Science Ltd., Hungary. However, two authors (ZK and ÁK) acted regularly as external scientific consultants for this company. In this role they were actively involved in scaling up titanate nanomaterial production to a commercial scale in the Auro-Science plant.

$Na_2Ti_3O_7$, sodium metatitanate is registered in CAS as 12034-36-05 and is available commercially from all major lab chemical vendors without any morphology specification. Typical fine chemical prices are in the range of 3000 USD kg^{-1}.

The world market of layered titanate nanomaterials has only started developing recently. It is a demand-driven market where buyers are waiting for demonstrations of the specific benefits this material can offer over the well-known and abundant nanosized TiO_2 powder. Titanate nanotubes are sold as CAS 12026-28-7 (metatitanic acid) by commercial nanotube suppliers (e.g. Auro-Science Ltd in Hungary, Smart Metal Limited, Xuzhou Jiechuang New Material Technology Co, JinZhongYan New Material Technology Co. and Hongwu International Group Ltd. in China), with an estimated combined capacity of 4000 metric tons per year [146, 147]. Prices range from 150 to 250 USD kg^{-1} for pristine titanate nanotubes and can be significantly higher for functionalized and/or modified samples. Titanate nanowires are cheaper to manufacture than nanotubes because they can be produced in larger batches. The only dedicated commercial manufacturer of titanate nanowires in the world today is Auro-Science Ltd, Hungary[5] [148].

Titanate nanotubes and nanowires stand out from the sea of diverse nanomaterials developed in the past two decades because it is actually feasible to scale their synthesis up and produce them on a commercial scale at reasonable cost. This is possible because of the following advantages:

(a) They are obtained with close to 100% yield as the TiO_2 raw material recrystallizes in the alkaline hydrothermal process. Conversion is 100% because titanates are thermodynamically favored over TiO_2 at those experimental conditions, and there are no by-products or alternative products.
(b) The synthesis method is robust. Minor variations in reaction temperature and time or a change in the TiO_2 supplier will not affect the product quality severely.
(c) The process in non-explosive, water based and has a very small environmental footprint. The only waste that leaves the plant is the brine formed upon the neutralization of $Na_2Ti_3O_7$ by diluted hydrochloric acid.
(d) Equipment wise, the core layered titanate nanomaterial synthesis technology is very similar to that of synthetic zeolite production. Therefore, existing zeolite plants could be converted into titanate nanomaterial sources with little cost, thus supply will likely be able to keep up with growing demand in the foreseeable future.

Titanate nanostructures, in particular, titanate nanotubes are obtained as a fluffy white monolith even in a pilot scale autoclave. There is a big difference in the apparent density of the raw material TiO_2 and the produced nanotubes, therefore, it is difficult to optimize the batch size. Moreover, the viscosity of the system changes considerably from the start of the synthesis (TiO_2 powder + NaOH solution) to the end ($Na_2Ti_3O_7$ monolith) and this must be considered when designing the autoclave. The third factor complicating industrial scale production is the necessity of using special equipment (e.g. nickel plated, Teflon coated or enameled autoclave) that can cope with the highly concentrated alkaline solutions involved.

Unlike most chemicals, titanate nanotubes and nanowires do not have an infinite shelf life. Sodium metatitanate is the thermodynamically favored phase under the alkaline hydrothermal conditions of the synthesis, but this is no longer the case under ambient conditions. Therefore, layered titanates must be either stabilized or used a few months after synthesis because they can gradually transform into other phases as discussed above. The rate of the transformation depends largely on the exact manufacturing and storage conditions (e.g. Na^+:H^+ ratio, moisture content). Lines of future research on non-perovskite titanate nanomaterial commercialization should focus on the following areas:

(a) Improving shelf life by e.g. partial ion exchange, polymer wrapping or nanocomposite formation.
(b) Broadening the scope of applications, with an emphasis on identifying fields where titanates can outperform TiO_2 or offer functions unavailable in TiO_2.
(c) Developing new synthesis machinery to circumvent the issues arising from the viscosity variation of the lye during the hydrothermal recrystallization. Solutions considered today are e.g. fixed bed lye-recirculating units and pressurized tandem mixers.

5. Applications

5.1. Battery and supercapacitor electrodes

The high specific surface area (<400 $m^2 \cdot g^{-1}$), electrical and ion conductivity as well as available space (0.65–0.85 nm) between the lamellae (or rolled up sheets) of layered titanates [128] have motivated a considerable effort to implement these materials as anodes in lithium batteries. Although capable of storing less Li^+ per mass of electrode than the widely used graphite (or other carbonaceous electrode materials) and having high redox potential (1.55 V) versus Li^+/Li, both limiting the overall energy storage compared to graphite, titanates offer several benefits that make such materials practical for commercialization. One of the main motives for replacing the affordable and abundant carbon based electrodes is the significant improvement in reliability and lifetime since titanates are less prone to

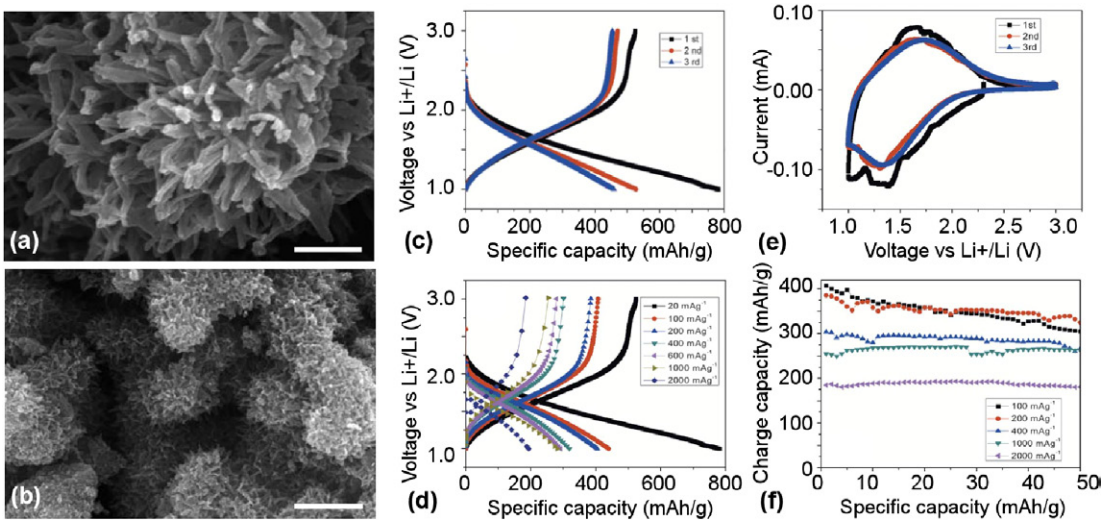

Figure 3. SEM images of lepidocrocite-type titanate nanowires (*a*, *b*). Panels (*c*) and (*d*) show the potential-capacity profiles at the charge/discharge current density of 20 mA · g^{-1} (repeated 3 times) and at various current densities between 20 and 2000 mA · g^{-1}, respectively. Cyclic voltammetry curve (*e*) and the cycling performance at different current densities (*f*). Reproduced from [159] with permission of the Royal Society of Chemistry.

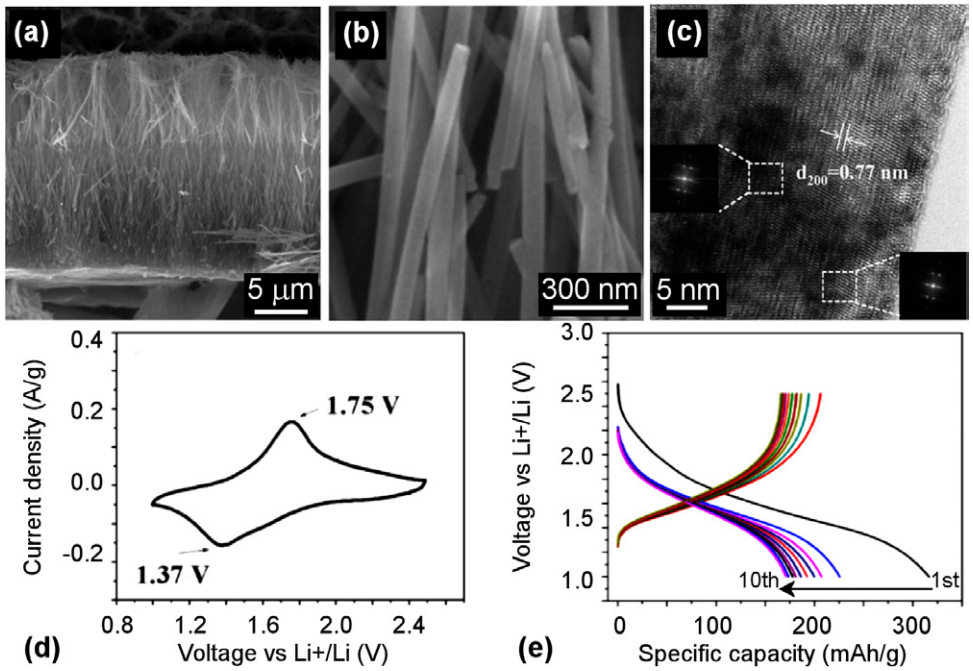

Figure 4. SEM (*a*, *b*) and TEM (*c*) images of $H_2Ti_2O_5$ nanowire arrays synthesized directly on the surface of a Ti foil by the hydrothermal method in 1 M NaOH aqueous solution at 220 °C for 24 h followed by soaking in 0.5 M HCl solution for 2 h to replace Na^+ of $Na_2Ti_2O_5$ with H+ thus forming $H_2Ti_2O_5$. Panels (*d*) and (*e*) show the corresponding cyclic voltammetry and charge-discharge curves at 0.1 C for the first ten cycles, respectively. Reproduced from [157]. Copyright 2014 American Chemical Society.

structural degradation and device failure because of their lesser volumetric change upon charging–discharging cycles. Another advantage of titanates over carbon is the eliminated Li dendrite formation on the anode material upon charging, thus reducing the risk of short circuiting and consequently improving safety [149].

Over the past 10 years, a number of different phases of 1D titanates such as $M_xH_{2-x}Ti_yO_{y+1}$ (M^I denotes Na or K, and the value of *y* is 2 [150–152], 3 [153], 4 [154], 6 [155, 156], and 8 [151, 157, 158]), lepidocrocites $H_xTi_{2-x/4}\square_{x/4}O_4 \times H_2O$ ($x \sim 0.7$, $\square$ is vacancy) [159, 160], spinel-type structures such as $Li_2M^{II}Ti_3O_8$ (M^{II} denotes Co, Zn or Mg) [161], $Li_4Ti_5O_{12}$ [95, 162–165] and $Li_2Na_2Ti_6O_{14}$ [166], as well as TiO_2(B) phase [167] have been demonstrated as excellent platforms for reversible Li ion intercalation with high specific charge storage capacity (figure 3). In typical experiments, the anode (negative electrode) is comprised of the actual titanate powders mixed with 5–15% binder (PVDF, PTFE) and 10–45% porous conductive filler (carbon black, carbon nanotubes), which is cast or stencil printed on metallic foils (Cu or Al). The counter electrode (cathode) is a Li foil. For electrolytes, usually

lithium hexafluorophosphate ($LiPF_6$), 1 M lithium perchlorate ($LiClO_4$) in a mixture of ethylene carbonate (EC), propylene carbonate (PC), dimethyl carbonate (DMC), ethyl methyl carbonate (EMC) and their mixtures are applied. The performance of layered titanate based electrodes is quite promising considering the initial discharge capacity of 800–200 mA · h · g^{-1} at a corresponding current density of 20–2000 mA · g^{-1}, and reversible capacity of ~300 mA · h · g^{-1} reported for the best materials (hydrogen titanates) [157]. The operation voltage range of the cells is between 2.5–1.0 V (the working electrode versus the Li electrode) resulting in an energy density that renders titanates indeed suitable for electrodes. Although most of the aforementioned phases fulfill the basic demands for reversible Li^+ intercalation, the insignificant volumetric change in spinels is very appealing from a practical point of view; however the low ion mobility in the structures compared to layered titanates may set a trade-off.

Another appealing approach for obtaining titanate based electrodes has been demonstrated by using titanate forests directly grown on the surface of titanium foils using practically the same route as known from the hydrothermal synthesis of titanate nanowires and nanotubes from titania in alkaline media (figure 4). The benefit of the method is the direct and intimate electrical interface and the ordered pore structure allowing simplified device integration and easy ion transport from/to the electrodes, respectively [157].

When using the titanate working electrodes with similar titanate or carbon counter electrodes instead of Li metal, the cell assemblies can be operated as supercapacitors and pseudocapacitors. Intercalation of titanates with Li^+ [168], Zn^{2+} [169], or Ni^{2+} [170] results in structures having specific capacitance of up to ~800 F · g^{-1}, energy density of 90 W · h · kg^{-1} and average power density of 11 000 W · kg^{-1} [171].

5.2. Adsorption and catalysis

Madarász *et al* have tested the water softening ability of titanate nanotubes in a fixed bed process simulating industrial usage [172]. The theoretical maximum ion exchange capacity for bivalent cations is 2.9 mmol · g^{-1} (taking into account the 10 wt% structural water content of the nanotubes) which is actually higher than that of a reference water softener resin DOWEX-50W. The highest ion exchange capacity achieved was 1.2 mmol · g^{-1} and this value dropped to 0.66 mmol · g^{-1} after two usage–regeneration cycles. The capacity loss was traced back to the irreversible binding of Ca^{2+} ions to the nanotubes.

Owing to their high specific surface, tunable acidity/basicity, and available/accessible cationic sites, adsorption of ionic pollutants from water has emerged as a straightforward application of titanates. In a similar working principle to clays and other layered minerals [173], protons and alkali cations in the layered titanates can be replaced by divalent ions of alkali-earth and transition metals. Considerable uptake of metal cations such as Cu^{2+} (up to 1.3 mmol · g^{-1}) and Pb^{2+} (up to 0.15 mmol · g^{-1}) on nanotubes [174], Ba^{2+} (up to 0.6 mmol · g^{-1}) and Sr^{2+} (up to 0.5 mmol · g^{-1}) on nanofibers [175], as well as Pb^{2+} (up to 1.5 mmol · g^{-1}) and mixtures of Cd^{2+}, Ni^{2+}, Zn^{2+} (total uptake of 1.5 mmol · g^{-1}) on titanate nanoflowers [176] show the remarkable potential of various titanates to tackle environmental, public and industrial water management. The reported ion adsorption capacity values in some cases even compete with those of chemically modified celluloses [177], commercial ion exchange resins [178] and activated carbon [179]. Because of the hydrophilic nature of the surface, selective adsorption of polar constituents from mixtures of polar and non-polar compounds is possible as it was shown by a selective chemisorption of nitrosamines on highly protonated titanates without reducing the amount of tar in cigarette smoke [180]. The hydrophilic behavior is also exploited in humidity sensors. The dielectric properties of titanates are highly sensitive to the adsorbed water due to the change in polarizability and ionic conduction in the lattice. Hence, by simple capacitance, conductance or dielectric spectroscopy analysis, it is possible to detect water content e.g. in ambient air [86, 181, 182].

Another interesting approach for humidity sensing combines water adsorption and simultaneous reversible dimerization of methylene blue dye being immobilized on titanate nanowires. In the presence of water, the titanate adsorbed dye undergoes dimerization forcing it to change molecular configuration and alignment on the surface in respect to dry conditions. The process results in a reversible change of the methylene blue color, allowing colorimetric humidity sensing. As the sensors can be integrated with optical fibers, the feasibility of the method is quite attractive for use in environmental monitoring and medical analysis [183].

Applications related to catalysis on titanates and their derivatives are associated mostly with chemical reactions (e.g. catalytic mitigation and oxidation of CO and organic pollutants, selective reduction of NO and activation of CO_2) often carried out on titania based catalytic systems. In most of the reports, the catalyst metals are deposited on the support using the same methods (precipitation and impregnation techniques) as applied for titania particles, and also the catalytic behavior of titanate supported catalysts are typically referenced to their TiO_2 based counterparts. Being chemically different materials, it is not a surprise that under identical reaction conditions, various phases of titania performance are different from those of the titanates and even these latter ones display rather dissimilar features due to their differences in stoichiometry, surface area and pore structure. As concluded in the reports, the differences in specific surface areas might correlate with the activity, however the major governing factor of reaction kinetics for the catalyzed reactions is actually the basicity of the support.

Ru catalyst on protonated $Na_2Ti_5O_5 \times H_2O$ nanotubes and $K_2Ti_8O_{17}$ nanowires in catalytic wet air oxidation of p-hydroxybenzoic acid was studied in reference to the classical P25 TiO_2. The considerably higher initial reaction rates measured on the Ru-titanate nanowires (0.29 mmol $\cdot$ g^{-1} min^{-1}) and (0.16 mmol $\cdot$ g^{-1} $\cdot$ min^{-1}) than on Ru-TiO_2 nanoparticles (0.09 mmol $\cdot$ g^{-1} $\cdot$ min^{-1}) correlated with the differing specific surface area of the support materials (285 m^2 $\cdot$ g^{-1}, 183 m^2 $\cdot$ g^{-1} and 80 m^2 $\cdot$ g^{-1}, respectively).

Au, Rh [184] and their bimetallic forms [185] on titanate nanowires and nanotubes were studied in detail for structure, their surface adsorption (CO, CO_2 and ethanol) and CO_2 activation properties in high vacuum experiments [186]. Although the morphology of the Au, Rh and bimetallic Au-Rh core-shell cluster were found independent of the presence of alkali adatoms on titanate nanowires, the catalytic activity of alkali impurities in titanate and titania supported metal nanoparticles show differences. For instance, Pd on $K_2Ti_6O_{13}$ tested for NO reduction in H_2 showed lower conversion values for NO below ~160 °C than that over Pd on TiO_2 (although similar values were measured above 160 °C), the selectivity of the reaction towards N_2 was about two times higher on the titanate based catalyst than on the titania counterpart in the entire temperature range (with an ~80% versus ~40% maximum value at ~160 °C). Similar alteration of the catalytic activity in citral hydrogenation reactions was observed due to the presence of Na^+ impurities (~3 wt.%) in the support using Pt and Pt-Sn catalyst nanoparticles deposited on calcined (600 °C) hydrogen titanates [187]. In this case, the alkali impurities caused higher citral conversion rates and considerably better selectivity for citronellal and dimethyloctanol products. A similar promoting effect of alkaline metals in reference to TiO_2 was reported for $Na_2Ti_3O_7$, $K_2Ti_6O_{13}$, and $Cs_2Ti_6O_{13}$ supported Ru catalyst in the ammonia decomposition reaction [188]. Although the specific surface area values of titanates were about two-fold compared to the TiO_2 support, which may explain their better catalytic activity, the very significant increase of reaction rates (~0.03 $mol_{NH3} \cdot mol_{Ru}^{-1} \cdot s^{-1}$, ~0.05 $mol_{NH3} \cdot mol_{Ru}^{-1} \cdot s^{-1}$ and ~0.16 $mol_{NH3} \cdot mol_{Ru}^{-1} \cdot s^{-1}$) in the order of $Na_2Ti_3O_7 < K_2Ti_6O_{13} < Cs_2Ti_6O_{13}$ suggest that it is the alkalinity of the supports that plays the most important role in their catalytic properties.

5.3. Photo(electro)catalytic activity

The well-known work of Fujishima and Honda published more than 40 years ago on photoelectrochemical water splitting [189] on TiO_2 surface has initiated a global research effort to exploit photons for producing fuels. In terms of water splitting, the process itself has rather limited economic use even if light of solar origin is used. Although many papers claim water splitting on TiO_2, which has scientific importance for sure, its overall power efficiency is very far from what one could get with the cheapest polymer based solar panels, not to mention the advanced multijunction inorganic cells with efficiency over 40%. In the case of other photocatalytic or photoelectrocatalytic reactions, however, the situation is different. For instance, considering the applications associated with self-cleaning and antimicrobial surfaces, air and water purification, selective photooxidation/reduction of hydrocarbons and alcohols, oxidation of CO or reduction of CO_2, among many others, the overall benefit can justify the use of photocatalysis even in conjunction with artificial light sources. Of course the most ideal source would be the Sun with its average irradiance of ~1 kW $\cdot$ m^{-2} on the Earth's surface in a broad spectral range from UV up to the far-IR wavelengths.

Now, let us consider the optical properties of titania and titanates. The wide band gap of titania (~3.2 eV) [9] indicates that the material is not going to be particularly photoactive in the visible and IR light due to the lack of band to band optical absorption above ~390 nm. Titanates have even wider band gap values as reported for $K_2Ti_6O_{13}$ nanotubes (3.4 eV and 3.5 eV) [68, 69] as well for sheets of 2D flakes (~3.8 eV) derived from lepidicrocite ($H_{0.7}Ti_{1.825}\square_{0.175}O_4 \times H_2O$) nanotubes (3.3 eV) [52] which means that the absorption edge can be quite deep in the UV. Although water splitting on 1D titanates has been demonstrated [190], the typical photo(electro)catalytic applications of these materials are oxidation and mineralization of organic compounds such as acetone [52], benzol [71], dehydrogenation (reforming) of alcohols [191], antibacterial flow through membranes [192], photocathodic protection of steel surfaces [193], and even electrodes for dye sensitized solar cells were shown as alternatives to TiO_2 electrodes [194].

1D titanates on the other hand are suitable starting materials for the synthesis of various titania phases by easy to scale and relatively simple annealing processes which dehydrates and gradually recrystallizes the titanate into titania [195]. Depending on the number of alkaline cations in the original titanate lattice, as well as on the temperature and duration of the annealing step either TiO_2-B, anatase, rutile, their heterogeneous composites or even some core-shell type hierarchical structures of nanowires can form [196–198]. It is important to point out that the band gap of titanate nanowires/nanotubes decreases and reaches that of TiO_2 during recrystallization as the titanate gradually transforms to titania [199]. Therefore, such titania nanowires inherit all the advantages of the elongated structures from the titanate nanowires/nanotubes [66], and in addition have better optical absorption and thus more efficient electron–hole pair generation than in the original titanates.

In practice, the as-obtained titania nanowires are doped either by cations or anions, both leading to a decreased band gap and further improvement in the optical absorbance as new energy levels appear in the forbidden band giving rise to band to band transitions with lower energies. (Note: doping with F^- in the anionic sites is an exception, as energy levels from the lower edge of the conduction band disappear, thus the apparent band gap increases.) [128, 200–202] While doping improves photogeneration by shifting the absorption edge towards the more visible

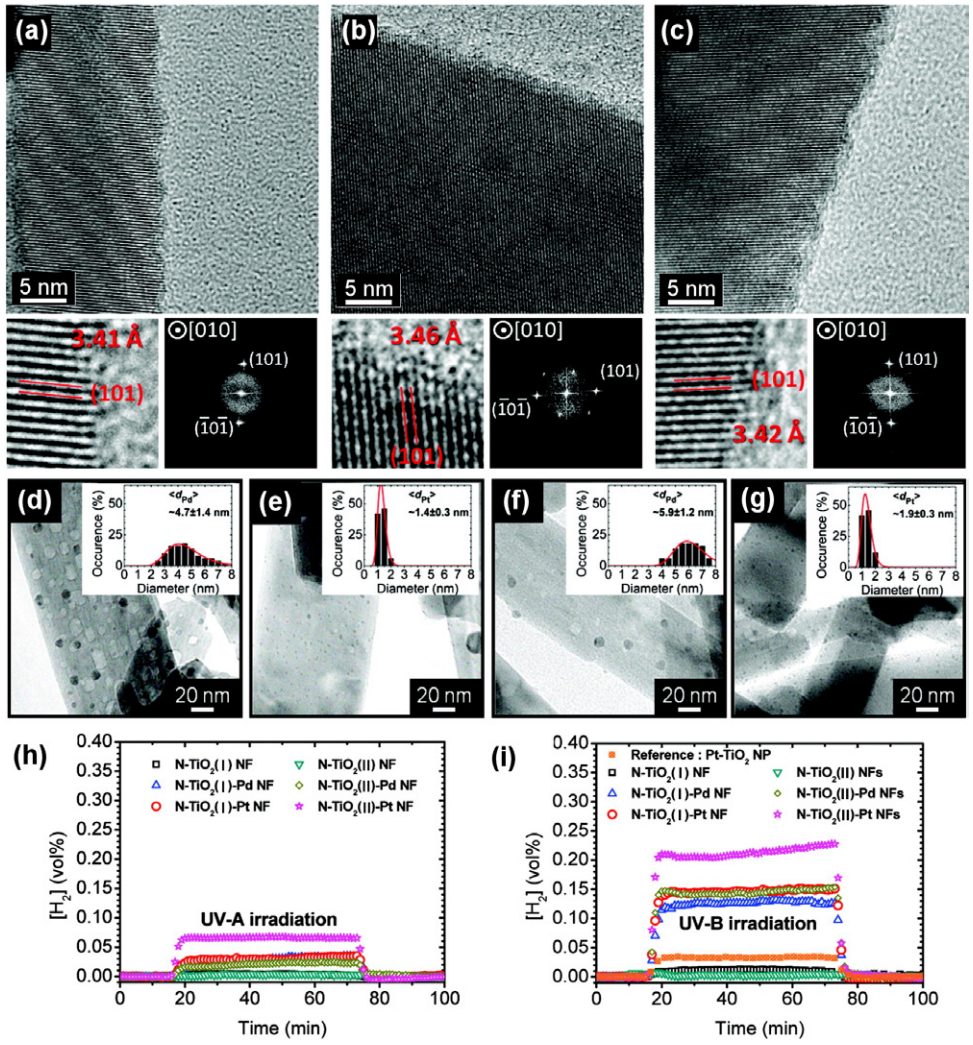

Figure 5. HR-TEM images of (*a*) pristine and (*b*, *c*) N-doped TiO_2 nanofibers obtained after annealing acid washed sodium titanate nanofibers in NH_3. Images (*d*)–(*g*) display TEM micrographs of N-doped and then Pd or Pt decorated NFs with metal loading of approx. 1.0 wt%. Panels (*h*) and (*i*) show hydrogen evolution from ethanol/water mixture (molar ratio 1:3) over the corresponding photocatalyst materials under UV-A and UV-B irradiation, respectively. Reproduced from [123]. Copyright 2011 American Chemical Society.

spectral region, it has no direct effect on the separation of electron–hole pairs, which would be vital for redox reactions to take place on the surface of the photocatalyst. The most frequently applied strategy for electron–hole separation is the formation of rectifying interfaces between the photocatalyst and a co-catalyst. The interface of metal nanoparticles (most common ones are Ni, Ag, Pd, Ti, Au) deposited on the surface of the semiconducting titanate and titania nanowires is actually a Schottky contact, which can rectify electron injection from the conduction band of the semiconductor to the Fermi level of the metal due to the presence of a barrier from the opposite direction. Thus the photogenerated electrons in the semiconductor will be eventually trapped in the metal and consumed to reduce moieties adsorbed on the surface of the metal. The metals of high work function listed above play another important role, which is more for the chemistry than for the physics. It is their catalytic activity in a common sense, known to be promoting chemical reduction [123, 203, 204] (figure 5). On the other hand, the holes left behind in the semiconductor will participate in oxidative processes, which can be promoted by other co-catalysts (e.g. CoO_x, $CaMn_xO_y$) added onto the surface of the semiconductor.

5.4. Bioactive surfaces and scaffolds

Ideally, bioscaffolds are porous materials that combine pores of multiple dimensions. The macropores, i.e. millimeter and micrometer size voids in the skeletal structures are responsible for nutrition and side-product transport to/from the cells as well as for the accommodation of cell colonies, while meso and micropores ensure optimal attachment and proliferation of cells [205]. In addition, the surfaces are expected to have a hydrophilic nature to allow reasonable bonding of the biological matter (H-bonding, dipole-dipole interaction) but at the same time, the surface should be rather inert to avoid coagulation of proteins and stress in cells. Titanate nanostructures directly grown on Ti or on its alloys [157, 205] with other metals are fulfilling all criteria listed

above thus are gradually becoming competitive alternatives [206–208] of the very popular conventional (e.g. polystyrene, polyethyleneterephtalate) and biodegradable polymers (e.g. poly(L-lactic acid), poly(DL-lactic-co-glycolic acid) [209–215].

Recently, titanate nanowires have been intensively studied as potential scaffolds for medical implants [205, 207–211]. Hydroxyapatite coated 1D titanate nanostructures were found to have high osteogenic, structural integrity and they show excellent mechanical performance. The main advantage of this material arises from its ability to mimic the natural extracellular matrix [207]. Besides their nanoscale structure, high specific surface area and chemical composition are two crucial attributes that make nanotitanates excellent candidates to be applied as bioscaffolds. Their ability to exchange ions (sodium or potassium to calcium) when soaked into simulated body fluids promotes the fast formation of biomaterials for e.g. apatite [208, 211]. 1D titanates grown inside the pores of the biocompatible 3D microporous Ti-based metal frames synthesized by low temperature hydrotermal treatment form a similar surface as the lowest levels of hierarchical organization of collagen and hydroxyapatite that enables cell attachment and proliferation [205]. Furthermore, due to the inherent photocatalytic behavior of titanates quick, easy and low cost sterilization processes could be applied to clean such implants before their utilization [206].

5.5. Miscellaneous applications

Based on their unique properties, titanate nanostructures are suggested to have many additional promising applications in the field of high-temperature thermoelectric conversion, super-hydrophilic coatings, field emission, and electrorheology. Today these applications are still dominated by perovskite titanates, but preliminary results with layered titanate nanostructures are already available [85, 216, 217].

Titanate nanotubes, $Na_{2-x}H_xTi_3O_7$, prepared by the alkali hydrothermal method have been shown to be promising candidates for high-temperature thermoelectric conversion owing to their high thermoelectric power ($302\,\mu V \cdot K^{-1}$ in the range of 745–1032 K), ultralow thermal conductivity ($0.55–0.75\,W \cdot m^{-1} \cdot K^{-1}$), and high electrical resistivity ($325–525\,\Omega \cdot m$) [218].

Few interesting studies based on dispersed titanate nanostructures [219, 220] have been reported in the field of electrorheology (ER) that could find use in for e.g. the automotive industry. Suspension of titanate nanotubes (TNTs) has shown reversible rheological changes under the exposure of an electric field. Recently, He *et al* demonstrated that, owing to their higher specific surface area and large aspect ratio, TNT-based ER fluids show a higher storage modulus compared to P25. In addition, having an arranged structure, titanate nanotube arrays could be also applied as self-cleaning or anti-fogging surfaces due to their super-hydrophlic properties and high optical transparency [221].

6. Summary

Layered titanate nanostructures are promising materials for the nanotechnology industry because they can be synthesized in commercial amounts by a scalable, environmentally benign and relatively cheap process. Moreover, they offer several chemical modification options through morphology-conserving phase transformations, ion exchange, doping, nanoparticle decoration and covalent functionalization. Their biggest drawbacks are the limited shelf life and the sensitivity of the fine structural details to the humidity of their surroundings. Although their current major fields of application are in ion exchange and photocatalysis, it is expected that energy storage applications will emerge soon.

Acknowledgment

The financial support of the Academy of Finland (project Optifu) and the Hungarian Research Fund projects OTKA NN 110676, NK 106234 and K 112531 is acknowledged.

References

[1] Barringer E A and Bowen H K 1982 Formation, packing, and sintering of monodisperse TiO_2 powders *J. Am. Ceram. Soc.* **65** C199–201
[2] Kasuga T, Hiramatsu M, Hoson A, Sekino T and Niihara K 1998 Formation of titanium oxide nanotube *Langmuir* **14** 3160–3
[3] Kasuga T, Hiramatsu M, Hoson A, Sekino T and Niihara K 1999 Titania nanotubes prepared by chemical processing *Adv. Mater.* **11** 1307
[4] Lee K, Mazare A and Schmuki P 2014 1D titanium dioxide nanomaterials: nanotubes *Chem. Rev.* **114** 9385–454
[5] Bavykin D V, Friedrich J M and Walsh F C 2006 Protonated titanates and TiO_2 nanostructured materials: synthesis, properties, and applications *Adv. Mater.* **18** 2807–24
[6] Zhao B, Lin L, Chen C and He D-N 2013 Research progress on crystal growth mechanism of titania/titanate nano-powder materials *J. Inorg. Mater.* **28** 683–90
[7] Pang Y L, Lim S, Ong H C and Chong W T 2014 A critical review on the recent progress of synthesizing techniques and fabrication of TiO_2-based nanotubes photocatalysts *Appl. Catal.* A **481** 127–42

[8] Wang L and Sasaki T 2014 Titanium oxide nanosheets: graphene analogues with versatile functionalities *Chem. Rev.* **114** 9455–86
[9] Bavykin D V and Walsh F C 2010 *Titanate and Titania Nanotubes: Synthesis, Properties and Applications* (Cambridge: RSC Publishing)
[10] Barnard A S and Zapol P 2004 Effects of particle morphology and surface hydrogenation on the phase stability of TiO_2 *Phys. Rev.* B **70** 235403
[11] Schaub R, Wahlstrom E, Ronnau A, Laegsgaard E, Stensgaard I and Besenbacher F 2003 Oxygen-mediated diffusion of oxygen vacancies on the TiO_2(1 1 0) surface *Science* **299** 377–9
[12] Mojic-Lante B, Djenadic R, Srdic V V and Hahn H 2014 Direct preparation of ultrafine $BaTiO_3$ nanoparticles by chemical vapor synthesis *J. Nanopart. Res.* **16** 2618
[13] Srdic V V and Djenadic R R 2005 Nanocrystalline titanate powders: synthesis and mechanisms of perovskite particles formation *J. Optoelectron. Adv. Mater.* **7** 3005–13
[14] Zhang M, Vilarinho P M, Miranda Salvado I M and Silva A 2011 Organic acids on the fabrication of sol–gel lead zirconate titanate fibers *Mater. Res. Bull.* **46** 1515–20
[15] Bai J and Zhou B 2014 Titanium dioxide nanomaterials for sensor applications *Chem. Rev.* **114** 10131–76
[16] Bai Y, Mora-Sero I, De Angelis F, Bisquert J and Wang P 2014 Titanium dioxide nanomaterials for photovoltaic applications *Chem. Rev.* **114** 10095–130
[17] Dahl M, Liu Y and Yin Y 2014 Composite titanium dioxide nanomaterials *Chem. Rev.* **114** 9853–89
[18] Sang L, Zhao Y and Burda C 2014 TiO_2 nanoparticles as functional building blocks *Chem. Rev.* **114** 9283–318
[19] Rorvik P M, Grande T and Einarsrud M-A 2011 1D nanostructures of ferroelectric perovskites *Adv. Mater.* **23** 4007–34
[20] Zhu X, Liu Z and Ming N 2010 Perovskite oxide nanotubes: synthesis, structural characterization, properties and applications *J. Mater. Chem.* **20** 4015–30
[21] Zhu X, Liu Z and Ming N 2010 Perovskite oxide nanowires: synthesis, property and structural characterization *J. Nanosci. Nanotechnol.* **10** 4109–23
[22] Ma R Z, Bando Y and Sasaki T 2003 Nanotubes of lepidocrocite titanates *Chem. Phys. Lett.* **380** 577–82
[23] Yang J J, Jin Z S, Wang X D, Li W, Zhang J W, Zhang S L, Guo X Y and Zhang Z J 2003 Study on composition, structure and formation process of nanotube $Na_2Ti_2O_4(OH)_2$ *Dalton Trans.* 3898–901
[24] Nakahira A, Kato W, Tamai M, Isshiki T, Nishio K and Aritani H 2004 Synthesis of nanotube from a layered $H_2Ti_4O_9{\cdot}H_2O$ in a hydrothermal treatment using various titania sources *J. Mater. Sci.* **39** 4239–45
[25] Armstrong G, Armstrong A R, Canales J and Bruce P G 2005 Nanotubes with the TiO_2-B structure *Chem. Commun.* 2454–6
[26] Ma R Z, Fukuda K, Sasaki T, Osada M and Bando Y 2005 Structural features of titanate nanotubes/nanobelts revealed by Raman, x-ray absorption fine structure and electron diffraction characterizations *J. Phys. Chem.* B **109** 6210–4
[27] Saponjic Z V, Dimitrijevic N M, Tiede D M, Goshe A J, Zuo X B, Chen L X, Barnard A S, Zapol P, Curtiss L and Rajh T 2005 Shaping nanometer-scale architecture through surface chemistry *Adv. Mater.* **17** 965
[28] Kubota Y, Kurata H and Isoda S 2006 Nanodiffraction and characterization of titanate nanotube prepared by hydrothermal method *Mol. Cryst. Liq. Cryst.* **445** 107–13
[29] Wu D, Liu J, Zhao X N, Li A D, Chen Y F and Ming N B 2006 Sequence of events for the formation of titanate nanotubes, nanofibers, nanowires, and nanobelts *Chem. Mater.* **18** 547–53
[30] Chen Q and Peng L M 2007 Structure and applications of titanate and related nanostructures *Int. J. Nanotechnol.* **4** 44–65
[31] Jitputti J, Rattanavoravipa T, Chuangchote S, Pavasupree S, Suzuki Y and Yoshikawa S 2009 Low temperature hydrothermal synthesis of monodispersed flower-like titanate nanosheets *Catal. Commun.* **10** 378–82
[32] Yu S-H, Park M, Kim H S, Jin A, Shokouhimehr M, Ahn T-Y, Kim Y-W, Hyeon T and Sung Y-E 2014 2D assemblies of ultrathin titanate nanosheets for lithium ion battery anodes *RSC Adv.* **4** 12087–93
[33] Kukovecz A, Hodos N, Horvath E, Radnoczi G, Konya Z and Kiricsi I 2005 Oriented crystal growth model explains the formation of titania nanotubes *J. Phys. Chem.* B **109** 17781–3
[34] Sui X-L, Wang Z-B, Li C-Z, Zhang J-J, Zhao L and Gu D-M 2014 Effect of pH value on $H_2Ti_2O_5/TiO_2$ composite nanotubes as Pt catalyst support for methanol oxidation *J. Power Sources* **272** 196–202
[35] Marinkovic B A, Fredholm Y C, Morgado E Jr, Jardim P M and Rizzo F 2010 Structural resistance of chemically modified 1D nanostructured titanates in inorganic acid environment *Mater. Charact.* **61** 1009–17
[36] Zhu K, Gao H, Hu G and Shi Z 2013 A rapid transformation of titanate nanotubes into single-crystalline anatase TiO_2 nanocrystals in supercritical water *J. Supercrit. Fluids* **83** 28–34
[37] Mao Y B and Wong S S 2006 Size- and shape-dependent transformation of nanosized titanate into analogous anatase titania nanostructures *J. Am. Chem. Soc.* **128** 8217–26
[38] Zhu H Y, Lan Y, Gao X P, Ringer S P, Zheng Z F, Song D Y and Zhao J C 2005 Phase transition between nanostructures of titanate and titanium dioxides via simple wet-chemical reactions *J. Am. Chem. Soc.* **127** 6730–6
[39] Kuo H-L, Kuo C-Y, Liu C-H, Chao J-H and Lin C-H 2007 A highly active bi-crystalline photocatalyst consisting of TiO_2 (B) nanotube and anatase particle for producing H_2 gas from neat ethanol *Catal. Lett.* **113** 7–12
[40] Morgado E Jr, Jardim P M, Marinkovic B A, Rizzo F C, De Abreu M A S, Zotin J L and Araujo A S 2007 Multistep structural transition of hydrogen trititanate nanotubes into TiO_2-B nanotubes: a comparison study between nanostructured and bulk materials *Nanotechnology* **18** 495710
[41] Cortes-Jacome M A, Ferrat-Torres G, Ortiz L F F, Angeles-Chavez C, Lopez-Salinas E, Escobar J, Mosqueira M L and Toledo-Antonio J A 2007 *In situ* thermo-Raman study of titanium oxide nanotubes *Catal. Today* **126** 248–55
[42] Li G, Liu Z-Q, Lu J, Wang L and Zhang Z 2009 Effect of calcination temperature on the morphology and surface properties of TiO_2 nanotube arrays *Appl. Surf. Sci.* **255** 7323–8
[43] Shokuhfar T, Gao Q, Ashtana A, Walzack K, Heiden P and Friedrich C 2010 Structural instabilities in TiO_2 nanotubes *J. Appl. Phys.* **108** 104301
[44] Xu H, Li C, He D and Jinag Y 2014 Stability and structure changes of Na-titanate nanotubes at high temperature and high pressure *Powder Diffr.* **29** 147–50
[45] Poudel B, Wang W Z, Dames C, Huang J Y, Kunwar S, Wang D Z, Banerjee D, Chen G and Ren Z F 2005 Formation of crystallized titania nanotubes and their transformation into nanowires *Nanotechnology* **16** 1935–40
[46] Zhao B, Lin L, Chen C, Chai Y and He D 2013 Research on the phase transition and morphological evolution behaviors of titania/titanate nanomaterials by calcination treatment *Acta Chim. Sin.* **71** 93–101
[47] Beuvier T, Richard-Plouet M and Brohan L 2010 Ternary morphological diagram for nano(tube-ribbon-sphere) sodium titanate deduced from Raman spectra analysis *J. Phys. Chem.* C **114** 7660–5
[48] Horvath E, Kukovecz A, Konya Z and Kiricsi I 2007 Hydrothermal conversion of self-assembled titanate nanotubes into nanowires in a revolving autoclave *Chem. Mater.* **19** 927–31
[49] Bavykin D V, Kulak A N and Walsh F C 2010 Metastable nature of titanate nanotubes in an alkaline environment *Cryst. Growth Des.* **10** 4421–7

[50] Kozma G, Konya Z and Kukovecz A 2013 Non-equilibrium transformation of titanate nanowires to nanotubes upon mechanochemical activation *RSC Adv.* **3** 7681–3
[51] Mogilevsky G, Chen Q, Kulkarni H, Kleinhammes A, Mullins W M and Wu Y 2008 Layered nanostructures of delaminated anatase: nanosheets and nanotubes *J. Phys. Chem.* C **112** 3239–46
[52] Gao T, Wu Q, Fjellvag H and Norby P 2008 Topological properties of titanate nanotubes *J. Phys. Chem. C* **112** 8548–52
[53] Schuerer B, Elser M J, Sternig A, Peukert W and Diwald O 2011 Delamination and dissolution of titanate nanowires: a combined structure and *in situ* second harmonic generation study *J. Phys. Chem.* C **115** 12381–7
[54] Wen P, Itoh H, Tang W and Feng Q 2008 Transformation of layered titanate nanosheets into nanostructured porous titanium dioxide in polycation solution *Micropor. Mesopor. Mater.* **116** 147–56
[55] Li Y, Gao X P, Li G R, Pan G L, Yan T Y and Zhu H Y 2009 Titanate nanofiber reactivity: fabrication of $MTiO_3$ (M = Ca, Sr, and Ba) perovskite oxides *J. Phys. Chem.* C **113** 4386–94
[56] Cao Y, Zhu K, Wu Q, Gu Q and Qiu J 2014 Hydrothermally synthesized barium titanate nanostructures from $K_2Ti_4O_9$ precursors: morphology evolution and its growth mechanism *Mater. Res. Bull.* **57** 162–9
[57] Bavykin D V, Parmon V N, Lapkin A A and Walsh F C 2004 The effect of hydrothermal conditions on the mesoporous structure of TiO_2 nanotubes *J. Mater. Chem.* **14** 3370–7
[58] Lee C-K, Fen S-K, Chao H-P, Liu S-S and Huang F-C 2012 Effects of pore structure and surface chemical characteristics on the adsorption of organic vapors on titanate nanotubes *Adsorption-J. Int. Adsorption Soc.* **18** 349–57
[59] Haspel H, Bugris V and Kukovecz A 2014 Water-induced changes in the charge-transport dynamics of titanate nanowires *Langmuir* **30** 1977–84
[60] Hong J, Cao J, Sun J Z, Li H Y, Chen H Z and Wang M 2003 Electronic structure of titanium oxide nanotubules *Chem. Phys. Lett.* **380** 366–71
[61] Bavykin D V, Gordeev S N, Moskalenko A V, Lapkin A A and Walsh F C 2005 Apparent 2D behavior of TiO_2 nanotubes revealed by light absorption and luminescence *J. Phys. Chem.* B **109** 8565–9
[62] Thorne A, Kruth A, Tunstall D, Irvine J T S and Zhou W Z 2005 Formation, structure, and stability of titanate nanotubes and their proton conductivity *J. Phys. Chem.* B **109** 5439–44
[63] Dittrich T, Weidmann J, Timoshenko V Y, Petrov A A, Koch F, Lisachenko M G and Lebedev E 2000 Thermal activation of the electronic transport in porous titanium dioxides *Mater. Sci. Eng.* B **69** 489–93
[64] Alonso Santos-Lopez I, Handy B E and Garcia-de-Leon R 2013 Titanate nanotubes as support of solid base catalyst *Thermochim. Acta* **567** 85–92
[65] Xu D, Li J, Yu Y and Li J 2012 From titanates to TiO_2 nanostructures: controllable synthesis, growth mechanism, and applications *Sci. China-Chem.* **55** 2334–45
[66] Ming-Chung W, Toth G, Sapi A, Leino A-R, Konya Z, Kukovecz A, Su W-F and Kordas K 2012 Synthesis and photocatalytic performance of titanium dioxide nanofibers and the fabrication of flexible composite films from nanofibers *J. Nanosci. Nanotechnol.* **12** 1421–4
[67] Zhou W, Liu H, Boughton R I, Du G, Lin J, Wang J and Liu D 2010 1D single-crystalline Ti–O based nanostructures: properties, synthesis, modifications and applications *J. Mater. Chem.* **20** 5993–6008
[68] Wang B, Shi Y and Xue D 2007 Large aspect ratio titanate nanowire prepared by monodispersed titania submicron sphere via simple wet-chemical reactions *J. Solid State Chem.* **180** 1028–37
[69] Du G H, Chen Q, Han P D, Yu Y and Peng L M 2003 Potassium titanate nanowires: structure, growth, and optical properties *Phys. Rev.* B **67** 035323
[70] Li Q, Kako T and Ye J 2010 Strong adsorption and effective photocatalytic activities of 1D nano-structured silver titanates *Appl. Catal.* A **375** 85–91
[71] Tang Z-R, Li F, Zhang Y, Fu X and Xu Y-J 2011 Composites of titanate nanotube and Carbon nanotube as photocatalyst with high mineralization ratio for gas-phase degradation of volatile aromatic pollutant *J. Phys. Chem.* C **115** 7880–6
[72] Riss A, Elser M J, Bernardi J and Diwald O 2009 Stability and photoelectronic Properties of Layered Titanate Nanostructures, *J. Am. Chem. Soc.* **131** 6198–206
[73] Wang D, Zhou F, Wang C, Liu W 2008 Synthesis and characterization of silver nanoparticle loaded mesoporous TiO_2 nanobelts *Micropor. Mesopor. Mater.* **116** 658–64
[74] Yu H G, Yu J G, Cheng B and Zhou M H 2006 Effects of hydrothermal post-treatment on microstructures and morphology of titanate nanoribbons *J. Solid State Chem.* **179** 349–54
[75] Lin C-H, Wong D S-H and Lu S-Y 2014 Layered protonated titanate nanosheets synthesized with a simple one-step, low-temperature, urea-modulated method as an effective pollutant adsorbent *ACS Appl. Mater. Interfaces* **6** 16669–78
[76] Wang J, Yin S and Sato T 2006 Characterization of $H_2Ti_4O_9$ with high specific surface area prepared by a delamination/reassembling process *Mater. Sci. Eng.* C **126** 53–8
[77] Chang M, Chung C C, Deka J R, Lin C H and Chung T W 2008 Mechanical properties of microwave hydrothermally synthesized titanate nanowires *Nanotechnology* **19** 025710
[78] Bo A, Zhan H, Bell J, Zhu H and Gu Y 2014 Mechanical bending properties of sodium titanate ($Na_2Ti_3O_7$) nanowires *RSC Adv.* **4** 56970–6
[79] Kukkola J, Kukovecz A and Kordas K 2015 unpublished
[80] Li S, Liu L, Tian D and Zhao H 2011 Synthesis and electrical properties of $Na_2Ti_3O_7$ nanoribbons *Micro Nano Lett.* **6** 233–5
[81] Matsuda A, Sakamoto H, Mohd Nor M A B, Kawamura G and Muto H 2013 Characterization and film properties of electrophoretically deposited nanosheets of anionic titanate and cationic MgAl-layered double hydroxide *J. Phys. Chem.* B **117** 1724–30
[82] Dong W, Cogbill A, Zhang T, Ghosh S and Tian Z R 2006 Multifunctional, catalytic nanowire membranes and the membrane-based 3D devices *J. Phys. Chem.* B **110** 16819–22
[83] Sun C, Wang N, Zhou S, Hu X, Zhou S and Chen P 2008 Preparation of self-supporting hierarchical nanostructured anatase/rutile composite TiO_2 film *Chem. Commun.* 3293–5
[84] Zhou W *et al* 2011 Nanopaper based on Ag/TiO_2 nanobelts heterostructure for continuous-flow photocatalytic treatment of liquid and gas phase pollutants *J. Hazardous Mater.* **197** 19–25
[85] Miyauchi M and Tokudome H 2006 Low-reflective and super-hydrophilic properties of titanate or titania nanotube thin films via layer-by-layer assembly *Thin Solid Films* **515** 2091–6
[86] Haspel H, Bugris V and Kukovecz A 2013 Water sorption induced dielectric changes in titanate nanowires *J. Phys. Chem. C* **117** 16686–97
[87] Madarasz D, Szenti I, Nagy L, Sapi A, Kukovecz A and Konya Z 2013 Fine tuning the surface acidity of titanate nanostructures *Adsorption-J. Int. Adsorption Soc.* **19** 695–700

[88] Kitano M, Nakajima K, Kondo J N, Hayashi S and Hara M 2010 Protonated titanate nanotubes as solid acid catalyst *J. Am. Chem. Soc.* **132** 6622
[89] Wada E, Kitano M, Nakajima K and Hara M 2013 Effect of preparation conditions on the structural and acid catalytic properties of protonated titanate nanotubes *J. Mater. Chem.* A **1** 12768–74
[90] Kitano M, Wada E, Nakajima K, Hayashi S, Miyazaki S, Kobayashi H and Hara M 2013 Protonated titanate nanotubes with Lewis and Bronsted acidity: relationship between nanotube structure and catalytic activity *Chem. Mater.* **25** 385–93
[91] Horvath E, Szilagyi I, Forro L and Magrez A 2014 Probing titanate nanowire surface acidity through methylene blue adsorption in colloidal suspension and on thin films *J. Colloid Interface Sci.* **416** 190–7
[92] Liu Y, Liu J, Yao W, Cen W, Wang H, Weng X and Wu Z 2013 The effects of surface acidity on CO_2 adsorption over amine functionalized protonated titanate nanotubes *RSC Adv.* **3** 18803–10
[93] Zhou Y K, Cao L, Zhang F B, He B L and Li H L 2003 Lithium insertion into TiO_2 nanotube prepared by the hydrothermal process *J. Electrochem. Soc.* **150** A1246–9
[94] Armstrong A R, Armstrong G, Canales J and Bruce P G 2005 TiO_2-B nanowires as negative electrodes for rechargeable lithium batteries *J. Power Sources* **146** 501–6
[95] Li J R, Tang Z L and Zhang Z T 2005 Controllable formation and electrochemical properties of 1D nanostructured spinel $Li_4Ti_5O_{12}$ *Electrochem. Commun.* **7** 894–9
[96] Wang B L, Chen Q, Wang R H and Peng L M 2003 Synthesis and characterization of $K_2Ti_6O_{13}$ nanowires *Chem. Phys. Lett.* **376** 726–31
[97] Yuan Z Y and Su B L 2004 Titanium oxide nanotubes, nanofibers and nanowires *Colloids Surf.* A **241** 173–83
[98] Menzel R, Peiro A M, Durrant J R and Shaffer M S P 2006 Impact of hydrothermal processing conditions on high aspect ratio titanate nanostructures *Chem. Mater.* **18** 6059–68
[99] Qamar M, Yoon C R, Oh H J, Kim D H, Jho J H, Lee K S, Lee W J, Lee H G and Kim S J 2006 Effect of post treatments on the structure and thermal stability of titanate nanotubes *Nanotechnology* **17** 5922–9
[100] Lee C-K, Wang C-C, Lyu M-D, Juang L-C, Liu S-S and Hung S-H 2007 Effects of sodium content and calcination temperature on the morphology, structure and photocatalytic activity of nanotubular titanates *J. Colloid Interface Sci.* **316** 562–9
[101] Morgado E Jr, de Abreu M A S, Moure G T, Marinkovic B A, Jardim P M and Araujo A S 2007 Effects of thermal treatment of nanostructured trititanates on their crystallographic and textural properties *Mater. Res. Bull.* **42** 1748–60
[102] Lee C-K, Lyu M-D, Liu S-S and Chen H-C 2009 The synthetic parameters for the preparation of nanotubular titanate with highly photocatalytic activity *J. Taiwan Inst. Chem. Eng.* **40** 463–70
[103] Hernandez-Alonso M D, Garcia-Rodriguez S, Sanchez B and Coronado J M 2011 Revisiting the hydrothermal synthesis of titanate nanotubes: new insights on the key factors affecting the morphology *Nanoscale* **3** 2233–40
[104] Thu Ha Thi V, Hang Thi A, Lien Thi T, Tuyet Mai Thi N, Thanh Thuy Thi T, Minh Tu P, Manh Hung D and Dinh L N 2014 Synthesis of titanium dioxide nanotubes via one-step dynamic hydrothermal process *J. Mater. Sci.* **49** 5617–25
[105] Dawson G, Chen W, Zhang T, Chen Z and Cheng X 2010 A study on the effect of starting material phase on the production of trititanate nanotubes *Solid State Sci.* **12** 2170–6
[106] Chau Thanh N, Falconer J L, Le Minh D and Yang W-D 2014 Morphology, structure and adsorption of titanate nanotubes prepared using a solvothermal method *Mater. Res. Bull.* **51** 49–55
[107] Ngamsinlapasathian S, Sakulkhaemaruethai S, Pavasupree S, Kitiyanan A, Sreethawong T, Suzuki Y and Yoshikawa S 2004 Highly efficient dye-sensitized solar cell using nanocrystalline titania containing nanotube structure *J. Photochem. Photobiol.* A **164** 145–51
[108] Bavykin D V, Cressey B A, Light M E and Walsh F C 2008 An aqueous, alkaline route to titanate nanotubes under atmospheric pressure conditions *Nanotechnology* **19** 275604
[109] Uchida S, Chiba R, Tomiha M, Masaki N and Shirai M 2002 Application of titania nanotubes to a dye-sensitized solar cell *Electrochemistry* **70** 418–20
[110] Morgado E Jr, de Abreu M A S, Pravia O R C, Marinkovic B A, Jardim P M, Rizzo F C and Araujo A S 2006 A study on the structure and thermal stability of titanate nanotubes as a function of sodium content *Solid State Sci.* **8** 888–900
[111] Bavykin D V and Walsh F C 2007 Kinetics of alkali metal ion exchange into nanotubular and nanofibrous titanates *J. Phys. Chem.* C **111** 14644–51
[112] Yada M, Inoue Y, Noda I, Morita T, Torikai T, Watari T and Hotokebuchi T 2013 Antibacterial properties of titanate nanofiber thin films formed on a titanium plate *J. Nanomater.* 476585
[113] Kukovecz A, Hodos M, Konya Z and Kiricsi I 2005 Complex-assisted one-step synthesis of ion-exchangeable titanate nanotubes decorated with CdS nanoparticles *Chem. Phys. Lett.* **411** 445–9
[114] Hodos M, Horvath E, Haspel H, Kukovecz A, Konya Z and Kiricsi I 2004 Photo sensitization of ion-exchangeable titanate nanotubes by CdS nanoparticles *Chem. Phys. Lett.* **399** 512–5
[115] Pusztai P, Puskas R, Varga E, Erdohelyi A, Kukovecz A, Konya Z and Kiss J 2014 Influence of gold additives on the stability and phase transformation of titanate nanostructures *Phys. Chem. Chem. Phys.* **16** 26786–97
[116] Oszko A, Potari G, Erdohelyi A, Kukovecz A, Konya Z, Kiricsi I and Kiss J 2011 Structure of the Au-Rh bimetallic system formed on titanate nanowires and nanotubes *Vacuum* **85** 1114–9
[117] Niu H, Cai Y, Shi Y, Wei F, Mou S and Jiang G 2007 Cetyltrimethylammonium bromide-coated titanate nanotubes for solid-phase extraction of phthalate esters from natural waters prior to high-performance liquid chromatography analysis *J. Chromatogr.* A **1172** 113–20
[118] Ma R Z, Sasaki T and Bando Y 2004 Layer-by-layer assembled multilayer films of titanate nanotubes, Ag- or Au-loaded nanotubes, and nanotubes/nanosheets with polycations *J. Am. Chem. Soc.* **126** 10382–8
[119] Jacimovic J, Horvath E, Nafradi B, Gaal R, Nikseresht N, Berger H, Forro L and Magrez A 2013 From nanotubes to single crystals: Co doped TiO_2 *APL Mater.* **1** 032111
[120] Wu D, Chen Y F, Liu J, Zhao X N, Li A D and Ming N B 2005 Co-doped titanate nanotubes *Appl. Phys. Lett.* **87** 112501
[121] Zhang W, Zhou W, Wright J H, Kim Y N, Liu D and Xiao X 2014 Mn-Doped TiO_2 nanosheet-based spheres as anode materials for lithium-ion batteries with high performance at elevated temperatures *ACS Appl. Mater. Interfaces* **6** 7292–300
[122] Hu C-C, Hsu T-C and Lu S-Y 2013 Effect of nitrogen doping on the microstructure and visible light photocatalysis of titanate nanotubes by a facile cohydrothermal synthesis via urea treatment *Appl. Surf. Sci.* **280** 171–8
[123] Wu M-C *et al* 2011 Nitrogen-doped anatase nanofibers decorated with noble metal nanoparticles for photocatalytic production of hydrogen *ACS Nano* **5** 5025–30
[124] Chang J-C, Tsai W-J, Chiu T-C, Liu C-W, Chao J-H and Lin C-H 2011 Chemistry in a confined space: characterization of nitrogen-doped titanium oxide nanotubes produced by calcining ammonium trititanate nanotubes *J. Mater. Chem.* **21** 4605–14
[125] Diaz-Guerra C, Umek P, Gloter A and Piqueras J 2010 Synthesis and cathodoluminescence of undoped and Cr^{3+}-doped sodium titanate nanotubes and nanoribbons *J. Phys. Chem.* C **114** 8192–8

[126] Song X C, Zheng Y F, Yin H Y and Cao G S 2005 Synthesis and characterization of transition element substituted titanate nanotubes *Acta Phys. Chim. Sin.* **21** 1076–80
[127] He X, Wang Z, Hirata A, Gu L, Chen M and Duan X 2011 Modulated $Na_2Ti_4O_9$:Zr nanobelt via site-specific Zr doping *Appl. Phys. Express* **4** 085003
[128] Asahi R, Morikawa T, Ohwaki T, Aoki K and Taga Y 2001 Visible-light photocatalysis in nitrogen-doped titanium oxides *Science* **293** 269–71
[129] Huang L, Sun Z and Liu Y 2007 N-doped TiO_2 nanotubes with visible light photo-activity for degradation of methyl orange in water *J. Ceram. Soc. Japan* **115** 28–31
[130] Feng C, Wang Y, Jin Z, Zhang J, Zhang S, Wu Z and Zhang Z 2008 Photoactive centers responsible for visible-light photoactivity of N-doped TiO_2 *New J. Chem.* **32** 1038–47
[131] Buchholcz B, Haspel H, Kukovecz A and Konya Z 2014 Low-temperature conversion of titanate nanotubes into nitrogen-doped TiO_2 nanoparticles *CrystEngComm* **16** 7486–92
[132] Han W-Q, Wen W, Yi D, Liu Z, Maye M M, Lewis L, Hanson J and Gang O 2007 Fe-doped trititanate nanotubes: formation, optical and magnetic properties and catalytic applications *J. Phys. Chem.* C **111** 14339–42
[133] Zhang Y, Han Y and Zhang L 2014 Characteriztion of Zn-doped TiO_2 nanotubes anodized on titanium surface *Rare Met. Mater. Eng.* **43** 68–71
[134] Jayabharathi J, Karunakaran C, Arunpandiyan A and Vinayagamoorthy P 2014 Styryl phenanthrimidazole-fluorescence switched on by core/shell $BaTiO_3$/ZnO and Mn-doped TiO_2/ZnO nanospheres and switched off by the core nanoparticles *RSC Adv.* **4** 59908–16
[135] Guo H, Chen J, Weng W, Zheng Z and Wang D 2014 Adsorption behavior of Congo red from aqueous solution on La_2O_3-doped TiO_2 nanotubes *J. Indust. Eng. Chem.* **20** 3081–8
[136] Milanovic M, Nikolic L M, Stijepovic I, Kontos A G and Giannakopoulos K P 2014 Steps in growth of Nb-doped layered titanates with very high surface area suitable for water purification *Mater. Chem. Phys.* **148** 874–81
[137] Tang Z-R, Zhang Y and Xu Y-J 2012 Tuning the optical property and photocatalytic performance of titanate nanotube toward selective oxidation of alcohols under ambient conditions *ACS Appl. Mater. Interfaces* **4** 1512–20
[138] Zhao W-R, Xi H-P and Liao Q-W 2013 Cu-doped titania nanotubes for visible-light photocatalytic mineralization of toluene *Acta Phys. Chim. Sin.* **29** 2232–8
[139] Kim D H, Lee K S, Yoon J H, Jang J S, Choi D-K, Sun Y-K, Kim S-J and Lee K S 2008 Synthesis and electrochemical properties of Ni doped titanate nanotubes for lithium ion storage *Appl. Surf. Sci.* **254** 7718–22
[140] Pedroni M, Piccinelli F, Polizzi S, Speghini A, Bettinelli M and Haro-Gonzalez P 2012 Upconverting Ho–Yb doped titanate nanotubes *Mater. Lett.* **80** 81–3
[141] Huskic M, Grguric T H, Umek P and Brnardic I 2013 Functionalization of sodium titanate nanoribbons with silanes and their use in the reinforcement of epoxy nanocomposites *Polym. Compos.* **34** 1382–8
[142] Lai Y *et al* 2011 Multi-functional hybrid protonated titanate nanobelts with tunable wettability *Soft Matter* **7** 6313–9
[143] Brnardic I, Huskic M, Umek P, Fina A and Grguric T H 2013 Synthesis of silane functionalized sodium titanate nanotubes and their influence on thermal and mechanical properties of epoxy nanocomposite *Phys. Status Solidi* A **210** 2284–91
[144] Ponton P I, d'Almeida J R M, Marinkovic B A, Savic S M, Mancic L, Rey N A, Morgado E Jr and Rizzo F C 2014 The effects of the chemical composition of titanate nanotubes and solvent type on 3-aminopropyltriethoxysilane grafting efficiency *Appl. Surf. Sci.* **301** 315–22
[145] Wang W, Zhang J, Huang H, Wu Z and Zhang Z 2008 Surface-modification and characterization of H-titanate nanotube *Colloids Surf.* A **317** 270–6
[146] Hongwu International Group Ltd www.hwnanomaterial.com
[147] Auro-Science Ltd http://auroscience.hu
[148] Nanobakt Ltd http://en.nanobakt.hu
[149] Carpenter N E 2014 *Chemistry of Sustainable Energy* (Boca Raton, FL: CRC Press)
[150] Zhang Y, Tang Y, Yin S, Zeng Z, Zhang H, Li C M, Dong Z, Chen Z and Chen X 2011 Hierarchical protonated titanate nanostructures for lithium-ion batteries *Nanoscale* **3** 4074–7
[151] Kim D H *et al* 2009 High electrochemical Li intercalation in titanate nanotubes *J. Phys. Chem.* C **113** 14034–9
[152] Xu R, Li J, Tan A, Tang Z and Zhang Z 2011 Novel lithium titanate hydrate nanotubes with outstanding rate capabilities and long cycle life *J. Power Sources* **196** 2283–8
[153] Li J R, Tang Z L and Zhang Z T 2005 Layered hydrogen titanate nanowires with novel lithium intercalation properties *Chem. Mater.* **17** 5848–55
[154] Suzuki S and Miyayama M 2010 Lithium intercalation properties of tetratitanates and octatitanates *J. Ceram. Soc. Japan* **118** 1154–8
[155] Perez-Flores J C, Kuhn A and Garcia-Alvarado F 2011 Synthesis, structure and electrochemical Li insertion behaviour of $Li_2Ti_6O_{13}$ with the $Na_2Ti_6O_{13}$ tunnel-structure *J. Power Sources* **196** 1378–85
[156] Zhang H, Gao X P, Li G R, Yan T Y and Zhu H Y 2008 Electrochemical lithium storage of sodium titanate nanotubes and nanorods *Electrochim. Acta* **53** 7061–8
[157] Liao J-Y, Xiao X, Higgins D, Lui G and Chen Z 2014 Self-supported single crystalline $H_2Ti_8O_{17}$ nanoarrays as integrated 3D anodes for lithium-ion microbatteries *ACS Appl. Mater. Interfaces* **6** 568–74
[158] Wang B L, Chen Q, Hu J, Li H, Hu Y F and Peng L M 2005 Synthesis and characterization of large scale potassium titanate nanowires with good Li-intercalation performance *Chem. Phys. Lett.* **406** 95–100
[159] Wu F, Wang Z, Li X and Guo H 2011 Hydrogen titanate and TiO_2 nanowires as anode materials for lithium-ion batteries *J. Mater. Chem.* **21** 12675–81
[160] Kang J-H, Paek S-M and Choy J-H 2012 Porous SnO_2/layered titanate nanohybrid with enhanced electrochemical performance for reversible lithium storage *Chem. Commun.* **48** 458–60
[161] Hong Z, Zheng X, Ding X, Jiang L, Wei M and Wei K 2011 Complex spinel titanate nanowires for a high rate lithium-ion battery *Energy Environ. Sci.* **4** 1886–91
[162] Lee D K, Shim H-W, An J S, Cho C M, Cho I-S, Hong K S and Kim D-W 2010 Synthesis of heterogeneous $Li_4Ti_5O_{12}$ nanostructured anodes with long-term cycle stability *Nanoscale Res. Lett.* **5** 1585–9
[163] Chen J, Yang L, Fang S and Tang Y 2010 Synthesis of sawtooth-like $Li_4Ti_5O_{12}$ nanosheets as anode materials for Li-ion batteries *Electrochim. Acta* **55** 6596–600
[164] Guerfi A, Charest P, Kinoshita K, Perrier M and Zaghib K 2004 Nano electronically conductive titanium-spinel as lithium ion storage negative electrode *J. Power Sources* **126** 163–8
[165] Hernandez V S, Martinez L M T, Mather G C and West A R 1996 Stoichiometry, structures and polymorphism of spinel-like phases, $Li_{1.33} \times Zn_{2-2x}Ti_{1+0.67x}O_4$ *J. Mater. Chem.* **6** 1533–6

[166] Yin S Y, Song L, Wang X Y, Huang Y H, Zhang K L and Zhang Y X 2009 Reversible lithium storage in $Na_2Li_2Ti_6O_{14}$ as anode for lithium ion batteries *Electrochem. Commun.* **11** 1251–4
[167] Zhang H, Li G R, An L P, Yan T Y, Gao X P and Zhu H Y 2007 Electrochemical lithium storage of titanate and titania nanotubes and nanorods *J. Phys. Chem.* C **111** 6143–8
[168] Yang J, Lian L, Xiong P and Wei M 2014 Pseudo-capacitive performance of titanate nanotubes as a supercapacitor electrode *Chem. Commun.* **50** 5973–5
[169] Hong Z and Wei M 2013 Layered titanate nanostructures and their derivatives as negative electrode materials for lithium-ion batteries *J. Mater. Chem.* A **1** 4403–14
[170] Zhou W, Liu X, Sang Y, Zhao Z, Zhou K, Liu H and Chen S 2014 Enhanced Performance of layered titanate nanowire-based supercapacitor electrodes by nickel ion exchange *ACS Appl. Mater. Interfaces* **6** 4578–86
[171] Wang Y, Hong Z, Wei M and Xia Y 2012 Layered $H_2Ti_6O_{13}$-nanowires: a new promising pseudocapacitive material in non-aqueous electrolyte *Adv. Funct. Mater.* **22** 5185–93
[172] Madarasz D, Szenti I, Sapi A, Halasz J, Kukovecz A and Konya Z 2014 Exploiting the ion-exchange ability of titanate nanotubes in a model water softening process *Chem. Phys. Lett.* **591** 161–5
[173] Carrol D 1959 Ion exchange in clays and other minerals *Geol. Soc. Am.* **70** 749–79
[174] Doong R-A and Chiang L-F 2008 Coupled removal of organic compounds and heavy metals by titanate/carbon nanotube composites *Water Sci. Technol.* **58** 1985–92
[175] Yang D, Zheng Z, Yuan Y, Liu H, Waclawik E R, Ke X, Xie M and Zhu H 2010 Sorption induced structural deformation of sodium hexatitanate nanofibers and their ability to selectively trap radioactive Ra(II) ions from water *Phys. Chem. Chem. Phys.* **12** 1271–7
[176] Huang J, Cao Y, Liu Z, Deng Z, Tang F and Wang W 2012 Efficient removal of heavy metal ions from water system by titanate nanoflowers *Chem. Eng. J.* **180** 75–80
[177] Hokkanen S 2014 *Modified Nano- and Microcellulose Based Adsorption Materials in Water Treatment* (Helsinki: School of Technology, Lappeenranta University of Technology) pp 207
[178] Lenntech www.lenntech.com/products/resins/ixresins.htm
[179] C.H. LLC www.buyactivatedcharcoal.com/heavy_metals_adsorption
[180] Deng Q, Huang C, Zhang J, Xie W, Xu H and Wei M 2013 Selectively reduction of tobacco specific nitrosamines in cigarette smoke by use of nanostructural titanates *Nanoscale* **5** 5519–23
[181] Haspel H, Laufer N, Bugris V, Ambrus R, Szabo-Revesz P and Kukovecz A 2012 Water-induced charge transport processes in titanate nanowires: an electrodynamic and calorimetric investigation *J. Phys. Chem.* C **116** 18999–9009
[182] Zhang Y *et al* 2008 A novel humidity sensor based on $Na_2Ti_3O_7$ nanowires with rapid response-recovery *Sensors Actuators* B **135** 317–21
[183] Horvath E, Ribic P R, Hashemi F, Forro L and Magrez A 2012 Dye metachromasy on titanate nanowires: sensing humidity with reversible molecular dimerization *J. Mater. Chem.* **22** 8778–84
[184] Kukovecz A, Potari G, Oszko A, Konya Z, Erdohelyi A and Kiss J 2011 Probing the interaction of Au, Rh and bimetallic Au-Rh clusters with the TiO_2 nanowire and nanotube support *Surf. Sci.* **605** 1048–55
[185] Kiss J, Ovari L, Oszko A, Potari G, Toth M, Baan K and Erdohelyi A 2012 Structure and reactivity of Au–Rh bimetallic clusters on titanate nanowires, nanotubes and TiO_2(1 1 0) *Catal. Today* **181** 163–70
[186] Toth M, Kiss J, Oszko A, Potari G, Laszlo B and Erdohelyi A 2012 Hydrogenation of carbon dioxide on Rh, Au and Au–Rh bimetallic clusters supported on titanate nanotubes nanowires and TiO_2 *Top. Catal.* **55** 747–56
[187] Rautio A-R, Maki-Arvela P, Aho A, Eranen K and Kordas K 2015 Chemoselective hydrogenation of citral by Pt and Pt–Sn catalysts supported on TiO_2 nanoparticles and nanowires *Catal. Today* **241** 170–8
[188] Klerke A, Klitgaard S K and Fehrmann R 2009 Catalytic ammonia decomposition over ruthenium nanoparticles supported on nanotitanates *Catal. Lett.* **130** 541–6
[189] Fujishima A and Honda K 1972 Electrochemical photolysis of water at a semiconductor electrode *Nature* **238** 37–8
[190] Yoshida H, Takeuchi M, Sato M, Zhang L, Teshima T and Chaskar M G 2014 Potassium hexatitanate photocatalysts prepared by a flux method for water splitting *Catal. Today* **232** 158–64
[191] Jang J S, Choi S H, Kim D H, Jang J W, Lee K S and Lee J S 2009 Enhanced photocatalytic hydrogen production from water-methanol solution by nickel intercalated into titanate nanotube *J. Phys. Chem.* C **113** 8990–6
[192] Shang L, Li B, Dong W, Chen B, Li C, Tang W, Wang G, Wu J and Ying Y 2010 Heteronanostructure of Ag particle on titanate nanowire membrane with enhanced photocatalytic properties and bactericidal activities *J. Hazardous Mater.* **178** 1109–14
[193] Zhu Y-F, Du R-G, Chen W, Qi H-Q and Lin C-J 2010 Photocathodic protection properties of 3D titanate nanowire network films prepared by a combined sol–gel and hydrothermal method *Electrochem. Commun.* **12** 1626–9
[194] Wei M D, Konishi Y, Zhou H S, Sugihara H and Arakawa H 2006 Utilization of titanate nanotubes as an electrode material in dye-sensitized solar cells *J. Electrochem. Soc.* **153** A1232–6
[195] Wu M-C *et al* 2011 Enhanced photocatalytic activity of TiO_2 nanofibers and their flexible composite films: Decomposition of organic dyes and efficient H_2 generation from ethanol-water mixtures *Nano Res.* **4** 360–9
[196] Thomas J and Yoon M 2012 Facile synthesis of pure TiO_2(B) nanofibers doped with gold nanoparticles and solar photocatalytic activities *Appl. Catal.* B **111** 502–8
[197] Mohl M *et al* 2014 Titania nanofibers in gypsum composites: an antibacterial and cytotoxicology study *J. Mater. Chem.* B **2** 1307–16
[198] Li W, Liu C, Zhou Y, Bai Y, Feng X, Yang Z, Lu L, Lu X and Chan K-Y 2008 Enhanced photocatalytic activity in anatase/TiO_2(B) core-shell nanofiber *J. Phys. Chem.* C **112** 20539–45
[199] Yu H, Yu J and Cheng B 2007 Photocatalytic activity of the calcined H-titanate nanowires for photocatalytic oxidation of acetone in air *Chemosphere* **66** 2050–7
[200] Xu M, Da P, Wu H, Zhao D and Zheng G 2012 Controlled Sn-doping in TiO_2 nanowire photoanodes with enhanced photoelectrochemical conversion *Nano Lett.* **12** 1503–8
[201] Chen X, Shen S, Guo L and Mao S S 2010 Semiconductor-based photocatalytic hydrogen generation *Chem. Rev.* **110** 6503–70
[202] Umebayashi T, Yamaki T, Itoh H and Asai K 2002 Analysis of electronic structures of 3D transition metal-doped TiO_2 based on band calculations *J. Phys. Chem. Solids* **63** 1909–20
[203] Wu M-C *et al* 2013 Photocatalytic activity of nitrogen-doped TiO_2-based nanowires: a photo-assisted Kelvin probe force microscopy study *J. Nanopart. Res.* **16** 2143
[204] Wu M-C, Liao H-C, Cho Y-C, Toth G, Chen Y-F, Su W-F and Kordas K 2013 Photo-Kelvin probe force microscopy for photocatalytic performance characterization of single filament of TiO_2 nanofiber photocatalysts *J. Mater. Chem.* A **1** 5715–20
[205] Wu S *et al* 2008 A biomimetic hierarchical scaffold: natural growth of nanotitanates on 3D microporous Ti-based metals *Nano Lett.* **8** 3803–8

[206] Dong W, Zhang T, Epstein J, Cooney L, Wang H, Li Y, Jiang Y-B, Cogbill A, Varadan V and Tian Z R 2007 Multifunctional nanowire bioscaffolds on titanium *Chem. Mater.* **19** 4454–9
[207] Zhao H, Dong W, Zheng Y, Liu A, Yao J, Li C, Tang W, Chen B, Wang G and Shi Z 2011 The structural and biological properties of hydroxyapatite-modified titanate nanowire scaffolds *Biomaterials* **32** 5837–46
[208] Liu Y X, Tsuru K, Hayakawa S and Osaka A 2004 Potassium titanate nanorod arrays grown on titanium substrates and their *in vitro* bioactivity *J. Ceram. Soc. Japan* **112** 634–40
[209] Sugiyama N *et al* 2009 Bioactive titanate nanomesh layer on the Ti-based bulk metallic glass by hydrothermal-electrochemical technique *Acta Biomater.* **5** 1367–73
[210] Ding X, Yang X, Zhou L, Lu H, Li S, Gao Y, Lai C and Jiang Y 2013 Titanate nanowire scaffolds decorated with anatase nanocrystals show good protein adsorption and low cell adhesion capacity *Int. J. Nanomed.* **8** 569–79
[211] Chen C-Y, Ozasa K, Katsumata K-i, Maeda M, Okada K and Matsushita N 2012 Bioactive titanium oxide-based nanostructures prepared by one-step hydrothermal anodization *J. Phys. Chem.* C **116** 8054–62
[212] Mikos A G, Lyman M D, Freed L E and Langer R 1994 Wetting of poly(L-lactic acid) and poly(Dl-lactic-Co-glycolic acid) foams for tissue-culture *Biomaterials* **15** 55–8
[213] Neff J A, Caldwell K D and Tresco P A 1998 A novel method for surface modification to promote cell attachment to hydrophobic substrates *J. Biomed. Mater. Res.* **40** 511–9
[214] Neff J A, Tresco P A and Caldwell K D 1999 Surface modification for controlled studies of cell-ligand interactions *Biomaterials* **20** 2377–93
[215] Yamamoto M, Kato K and Ikada Y 1997 Ultrastructure of the interface between cultured osteoblasts and surface-modified polymer substrates *J. Biomed. Mater. Res.* **37** 29–36
[216] Chakraborty I, Chatterjee S and Ayyub P 2011 Field emission from hydrogen titanate nanotubes *Appl. Phys. Lett.* **99** 143106
[217] Yin J, Zhao X, Xiang L, Xia X and Zhang Z 2009 Enhanced electrorheology of suspensions containing sea-urchin-like hierarchical Cr-doped titania particles *Soft Matter* **5** 4687–97
[218] Miao L, Tanemura S, Huang R, Liu C Y, Huang C M and Xu G 2010 Large Seebeck coefficients of protonated titanate nanotubes for high-temperature thermoelectric conversion *ACS Appl. Mater. Interfaces* **2** 2355–9
[219] He Y, Cheng Q, Pavlinek V, Li C and Saha P 2009 Synthesis and electrorheological characteristics of titanate nanotube suspensions under oscillatory shear *J. Indust. Eng. Chem.* **15** 550–4
[220] Yin J B and Zhao X P 2006 Titanate nano-whisker electrorheological fluid with high suspended stability and ER activity *Nanotechnology* **17** 192–6
[221] Miyauchi M and Tokudome H 2007 Super-hydrophilic and transparent thin films of TiO_2 nanotube arrays by a hydrothermal reaction *J. Mater. Chem.* **17** 2095–100